

Response to reviewer comments by Igor Polyakov	1
Response to reviewer comments by Marylou Athanase	16
Response to editor comment by Ilker Fer	22
References	22
Supplement	24
Track changes version	31

Response to reviewer comments by Igor Polyakov

Thank you very much for your very insightful second review and very constructive comments. We repeat your comments (using a dark red font color) below. Our responses are given in black font.

The authors made substantial revision of the original manuscript following the reviewers' comments. However, there are still several issues that need the authors' attention. They are related to the application of the methods and the quality of data processing and analysis. I think this study still requires major revision.

Comments:

1. Lines 3–4: The sentence is hard to read. Needs editing.

We split the sentence in two and replaced “based on” by “depending on” in order to avoid the awkward combination of “base” and “based on”. We also included the statement “unlike parameters previously used to detect the halocline base“ in order to emphasize the contrast to existing methods. The revised version reads:

Our main motivation for diagnosing the halocline base depth depending on vertical stability was that vertical stability is closely related to vertical mixing and heat exchange. Unlike parameters previously used to detect the halocline base, vertical stability is a crucial parameter for determining whether the halocline can prevent vertical heat exchange and protect sea ice from warm AW.

In an attempt to provide a more balanced discussion of pros and cons, we added the following sentence to the section describing the stability method (Sect. 2.3.1):

However, while vertical stability is closely related to vertical heat exchange and to the role of the halocline for protecting sea ice, the density ratio is more directly related to the original definition of a halocline.

2. Abstract: You can drop all abbreviations from the abstract if they are used only once. They will need to be defined in the text anyway.

Done. Thank you. We only retained AW for Atlantic Water because it is used in the abstract.

3. Lines 6-7: These two sentences can be merged.

Thank you for your suggestion. We omitted the first sentence.

4. Lines 10-13: The last two sentences do not belong to the end of Abstract. The authors may use GCM argument (ll. 9-10) to close this short discussion.

Thank you very much. We very much appreciate your suggestion. We moved both sentences up. We also slightly modified the new last sentence of the abstract because we noted an ambiguity. The original sentence was:

Comparatively large differences between the methods for detecting the halocline base depth were found in warm AW inflow regions for which climate models predict increased net surface energy fluxes from the ocean to the atmosphere, suggesting that these regions may be particularly sensitive to a halocline retreat.

In this original sentence, it was not entirely clear that the “*suggesting that*” refers to the analysis of model results mentioned in the second part of the sentence, and not to the large differences mentioned in the first part of the sentence. Therefore, we adapted the sentence as follows:

Comparatively large differences between the methods for detecting the halocline base depth were found in warm AW inflow regions for which climate models predict a halocline thinning and increased net surface energy fluxes from the ocean to the atmosphere.

5. Line 15. “Inflow regions” instead of “inflow”?

Yes, thank you. We replaced “inflow” by “inflow regions”.

6. Discussion of halocline formation (e.g. ll. 26-30 and throughout the text). Now the text reads as the freshwater capping is involved in and helps the halocline formation. It is partially true since the freshwater is the source for the density gradient in the halocline. But the formation of the halocline is driven by a) horizontal advection (injection) of denser water from shelves in winter and b) vertical mixing (overcoming stability of the surface fresher layer) due to winter sea ice formation and brine rejection. Thus, the physical drivers overcome stability of the water column to form the halocline.

Thank you very much. Based on a comments by both reviewers, we modified our discussion regarding the the interplay between convective homogenization and capping in the introduction of the manuscript. The revised part reads:

Based on data from the Oden 1991 cruise, Rudels et al. (1996) found that new halocline formation was initiated by the advection of relatively fresh shelf waters near the surface above denser and more saline water below, when the advection of the fresh water limited winter convection. Alkire et al. (2017) and Rudels et al. (2004) argued that convective homogenization and capping by fresh water due to sea ice melting in the inflow from the Fram Strait and the Barents Sea can transform AW into halocline water. Rudels et al. (2004) stressed that melting provides a precondition for sea ice formation and convective homogenization during the following winter.

We decided to omit the following sentence, which we deem less relevant in the light of our extended discussion on the roles of melt water:

Steele and Boyd (1998) argued that seasonal capping by melt water in summer may not be overly important for insulating the SML from relatively warm AW.

Throughout the manuscript, we now refer to the mechanisms that involve

convective homogenization and capping as “convective homogenization and capping” instead of simply “capping”.

7. Lines 36-37: Logic is broken in the LHW part, the sentence needs editing.

We added “not only in the Eurasian Basin but” to the LHW part of the sentence and also replaced the “but” in the beginning of this part by “while”. However, we are not sure if this addresses your concern. If not, could you please elaborate? Figure 5 of Polyakov et al. (2018) shows LHW below PHW extending to the Bering Shelf. Based on Anderson et al. (2013), we state that this LHW water is of Atlantic origin. Did we misinterpret this? The revised sentence reads:

The PHW in the Canada Basin originates from Pacific Water inflow, which is modified on the Chukchi Sea Shelf, while the LHW is of Atlantic origin not only in the Eurasian Basin but also in the Canada Basin (e.g. Anderson et al., 2013).

8. Lines 44-46: Editing is needed. It would be helpful if the authors would illustrate statements like that with figures.

We changed the lines as follows:

Below, we argue that an increase in salinity associated with the PWW and another increase associated with the LHW results in two distinct local stability maxima between the surface and the LHW (compare also schematic in Supplement 1 and profiles in Supplement 2).

referring to Figures in two newly added supplements. Below the next sentence (referring to the absence of the second stability maximum in the CHL in the Eurasian Basin), we added the sentence:

This allows us to identify the CHS.

The sentence referring to the CHS formed by Greenland melt water was moved to the end of the section.

9. Line 50: “ist”.

Thank you. We deleted the “t”, translating the German word “ist” (meaning “is”) into English.

10. Line 59, The authors may want to add reference to Shimadat etal 2006: K. Shimada, T. Kamoshida, M. Itoh, S. Nishino, E. Carmack, F. McLaughlin, S. Zimmermann, A. Proshutinsky, Pacific Ocean inflow: Influence on catastrophic reduction of sea ice cover in the Arctic Ocean. *Geophys. Res. Lett.* 33, L08605 (2006).

Done.

11. Line 98: This referencing to reviewers is not standard. I suggest to cut them.

We shortened the paragraph containing the manuscript outline as suggested by M. Athanase and and also cut the references to the reviews. But we did like the idea of citing the reviews in the text, and had initially found numerous arguments to defend our choice of citing the reviews.

12. Line 104: I suggest to change “In a halocline” to “in the Arctic halocline” and “must be” to “is”.

Thank you. Done.

13. Section 2.2. I suggest the authors illustrate these features using vertical profiles of temperature, salinity, and density. Means would probably work best.

In Section 2.2, we now refer to the schematic showing salinity and stability profiles (Supplement 1) and to profiles based on observations (Supplement 2) which we added in response to your comment #8 above. The salinity profile in the schematic is qualitatively similar to the profiles shown in figure 2 of Shimada et al. (2005). The salinity and stability profiles in the schematic are also qualitatively similar to the corresponding profiles in Figure 5a and d except for the layer of Pacific Summer

Water. They are also qualitatively similar to the corresponding profiles in Figure 5e and h except for the SML.

14. Line 152: “Halocline”, not “halcoline” (but sounds beautiful).

Thank you very much. We replaced “halcoline” by “halocline”. Although there appears to be no obvious meaning of the word halcoline, we hope that it may eventually be adapted for some purpose. In this event, any credit would have to be bestowed on Aagaard et al. (1981) who have discovered the word already more than 40 years before us ([https://doi.org/10.1016/0198-0149\(81\)90115-1](https://doi.org/10.1016/0198-0149(81)90115-1)).

15. Line 155: Please show this method using a profile.

We added Supplement 3 to explain the method using an example profile. Figure S3b illustrates the usage of the “moving maximum” operator.

16. Lines 156-163: Please show examples (profiles).

Supplement 3 contains three panels illustrating steps to determine the CHS bounds and center depth.

17. Line 167: Define “smoothed”.

We added the following sentence in line 163 of the revised manuscript (line 187 of the track changes version):

The smoothing was performed using a Gaussian filter as described in the next section.

18. Line 176: The authors need to cite the source, not our paper.

The revised statement reads as follows:

The accuracy of the sensors used for the ITP observations has been cited as 0.002°C for temperature and 0.002 for salinity (Polyakov et al., 2017)

in agreement with an assessment by the manufacturer (Janzen et al., 2016). For temperature, this accuracy range is supported by Wong et al. (2023a). For salinity, larger biases can arise due to sensor shift on longer time scales, depending on the manufacturing date of the sensor (Wong et al., 2023b)

Any further comments you may have on this are welcome.

19. Line 2003: Please define “slopes ... change”. They change everywhere, so the sentence is not clear.

We changed

please note that at ~170 m, the temperature and salinity slopes in Fig. 3a both change

to

please note the kink in the temperature and salinity profiles at ~170 m in Fig. 3a

20. Lines 203-206: This is a way too long sentence which can be easily split for 2-3.

The sentence starting in line 203 was split into two sentences.

21. Line 212: July 15 is not “After July”.

Thank you. We replaced “After” by “In”.

22. Figure 3: This new Figure and its analysis are my major concerns.

- a. Since density is used for the analysis, I suggest it is also shown.

Figures 3 and 5 of the revised manuscript include profiles of the potential density anomaly.

- b. I see a problem with the salinity profiles which show local minima just above the high gradient areas. It is a well-known problem and comes from data processing. It creates artificial instabilities (higher over lower salinity layers). I think that is partially the reason for the high level of noise in the density ratio profiles. This problem may affect all authors' results so it should be addressed properly. There are several ways to reduce the problem. One way is to use raw temperature and conductivity and use local correlations to better adjust the profiles. Probably, it will be prohibitively expensive time-/effort-wise. Another one is to apply smoothing, but it requires a lot of considerations. I suggest the authors consider that, fix the problem in the salinity profiles and describe it carefully in the text.

Figures in Supplement 4 and Supplement 6 correspond to Figures 3 and 5. But they are based on Level I instead of Level III data. We also found spurious halocline base depth minima in the DR and the TD method when analyzing data from coupled climate models (Metzner et al., 2020). Because there is no data assimilation involved in these model runs, these model results are not influenced by such data processing problems. We also argue that the spurious depth minima in Figures 4 and 5 are related to a layer of warm PWW. Such a layer may explain spurious detections of halocline base depth minima even in the absence of noise.

Please note that in Supplement 5 we included maps showing the locations of the profiles in Figure 3 together with maps of sea ice concentration based on Spreen et al. (2008).

- c. I am also wondering why the density ratio profiles change the sign from negative to positive within 60-170m whereas both temperature and salinity (as well as alpha and beta) are monotonic. I think within this depth range the density ratio should be positive. Please check. After fixing the problems described in b-c, the profiles and definitions (and further results!) may look differently.

The x-axis in the revised Figure 3c and h use cubic scaling (as explained in our answer to your next point). This makes it much easier to see where the density ratio changes sign. Where the gradients in Figure

3a are clearly positive and monotonic, the density ratio does not change sign. Isolated instances of negative density ratios do not cause the density ratio threshold to be exceeded because the density ratio threshold is an upper threshold.

- d. The authors may consider using log axis for the density ratio to show the 0.05 value.

We now use a cubic scaling (x^3) for the x-axis instead of $\log(x)$. $\log(x)$ changes sign and is undefined for negative values. Because $\log(x)$ changes sign, one cannot simply compute the absolute. Using $\log(x)$, one ends up with positive and negative values on both sides of the $x = 0$. A cubic scaling preserves the sign.

- e. (f-h) Why SML depth is at 130m? Density profile would help.

Figures 3c, h, m in the revised manuscript show the potential density anomaly. Vertical dotted lines show the surface potential density anomaly and the threshold value used to estimate the SML base depth.

- f. I suggest to use different colors for SML and CHL segments. If they occupy the same depth, one can barely separate them so both are clearly seen.

In addition to the different line styles, we now also use two different colors. We chose fairly dark colors because of their high contrast compared to the background.

- g. Overall figure structure: Instead of “I74,” I suggest to use general title “Methods” and subtitles for the three right columns using methods’ abbreviations.

Done.

- h. Caption: please define stability (and its unit). “threshold values,” “temperature difference” should be briefly explained.

Stability (L , unitless) was defined in Sect. 2.1.3. We added “(L , unitless, see Sect. 2.1.3)” to the caption of Figure 2 instead of Figure 3, because this is where stability is first shown in a figure.

23. Lines 219-222: The sentence needs editing.

We shortened the sentences:

This appears to be consistent with the mechanism for halocline formation described by Rudels et al. (1996). As stated above, Rudels et al. (1996) found new halocline formation taking place when relatively fresh shelf waters near the surface were advected above denser and saltier water below, limiting winter convection, while Rudels et al. (2004) and Alkire et al. (2017) stressed the role of melt water in general (including non-shelf water) in the warm Atlantic inflow through the Fram Strait and the Barents Sea for halocline formation via this type of capping mechanism.

to:

This appears to be consistent with the convective homogenization and capping mechanism for halocline formation described by Rudels et al. (1996).

24. Line 222: This sentence needs an explanation helping to see that “the convection affected halocline water” (e.g. ...”as expressed by ...”). There are many sentences throughout the text like that (e.g., lines 228, 229-230, etc.). The text will benefit from clarifying them.

We softened the statement in line 222 saying “Figure 2 suggests that in this particular case, the convection may have affected halocline water” and added the explanation: “because prior to the onset of convection, Fig. 2 shows a well-defined halocline”. We split the sentence previously starting in line 228 into two and explained that it is the identification of a stability maximum associated with fresh water near the surface that makes us think that the ST algorithm might capture the beginning of new

halocline formation (please refer to lines 226f of the revised manuscript or lines 255 of the track changes version).

25. Lines 236-237. This sentence (“Reasons..”) can be deleted.

Done.

26. Lines 240-250 etc. The authors often use reference to figures inside the sentences (e.g., ll. 242 twice, 246). Traditionally, however, these references are placed at the end of the sentences.

We moved the references to the end of the sentences in this part and in a few other instances.

27. Lines: 249-254: I disagree that the differences between these methods are in different direction of search. This is a very misleading explanation. I think the major reason is, as the authors rightly stressed prior to this paragraph, a better physical justification, reasoning for the ST method. I suggest to remove this discussion or edit providing a better explanation.

In the revised version, we clarified that this particular statement pertains to the robustness of the methods. We also added a sentence to support our conclusion that the search direction helps to explain a drastic reduction in the number of artifacts in the ST method compared to the other methods. We are convinced that looking at the different search directions provides a key for understanding the increased robustness of the ST method compared to both other methods. Although we did not mention this in the first draft of our manuscript, during the development of the ST method, we specifically changed the search direction in the ST method in order to reduce artifacts associated with the spurious detection of halocline base depth minima. Conversely, reversing the search direction in the ST method results in spurious halocline base depth minima.

28. Line 259: “The underlying grid...” – this sentence can be removed.

Done.

29. Figure 6: I suggest to remove panels f-j and corresponding text referencing it. In the Arctic Ocean, there are no differences. For d-e: How the differences were computed if the points in (a-c) were not occupying the same positions?

A drawback of the DR method is that it identifies a halocline base outside the Arctic Ocean in the Norwegian Sea. This becomes especially problematic as similar conditions to the ones encountered in the Norwegian Sea today may extent further north in the future. We think that a correct halocline identification in regions which are prone to changes is very important if an algorithm is to be used in a climate change context. In our opinion, masking out regions solely based on location is not a good idea in a situation in which water masses may change. This point is further explained in our answer to comment #32 below.

30. Lines 265-280: Please do not use negative definitions in describing the ST method. E.g. Line 266 states that the ST “overestimates” halocline depth compared with another method. That really reads as negative towards the ST.

The “overestimate” in lines 265–280 referred to the TD method. We replaced

while the TD method overestimates halocline depth relative to both other methods (Fig. 6b)

by:

while the TD method placed the halocline at greater depth compared to both other methods (Fig. 6b)

The statement:

This overestimate of the halocline base depth by the TD method compared to the other two methods is consistent ...

was adapted as follows:

This greater halocline base depth from the TD method compared to the other two methods is consistent ...

(Although we are slightly concerned that now this sounds like something “great” for the TD method).

The sentence from Sect. 3.2:

The more frequent halocline base depths larger than 120 m in the ST method are likely related to an overestimate of halocline base depth similar to the one found for the ST method for ITP-33 above.

was changed to:

The more frequent halocline base depths larger than 120 m in the ST method are likely related to a deeper halocline base similar to the one found for the ST method for ITP-33 above.

Finally, the sentence from Sect. 4:

In the Canada Basin, the new method overestimated the halocline base depth compared to the DR method, which correctly identified the halocline base for ITP-33.

was adopted as follows:

In the Canada Basin, the new method placed the halocline base deeper than the DR method, which correctly identified the halocline base for ITP-33.

31. Same text: I suggest you drop off the definition of regions using ovals. You may refer to the regions using their geographical names.

The reason for mentioning the elliptical regions is that we computed the summary statistics for the ellipses covering the regions.

32. Bottom of page 13: I strongly suggest that the authors drop off any mentioning of the Norwegian Sea since this is a very different region with very different water masses and driving forces. They can mask this area in Figs.

One of our goals was to design a robust method for detecting the cold halocline base which can be used in a climate change context in those regions which are most likely affected by climate change, and which may

actually shift as the Arctic either warms or cools. In a previous study, we found large differences in the Norwegian Sea and also the Greenland Sea between the DR and the TD method when comparing the frequency of halocline thinning events between climate model results for past and near present-day conditions. In our opinion, masking out regions solely based on location is not a good choice when investigating climate change because conditions are not stationary. We are especially concerned that conditions which were previously encountered only in the regions which were masked out may with time propagate into the part which initially was not masked out.

We added the following sentences to the first paragraph of Section 4:

Furthermore, the new ST algorithm does not require masking out pre-defined geographical regions based solely on their location. This is important because in a climate change context, the location of water masses may shift as the Arctic warms or cools.

33. Figure 7: Instead of “relative frequency” the authors may use “histogram”.

We have a slight preference for “relative frequencies” because a histogram can either show frequencies or relative frequencies.

34. Section 3.3: Lines 312-319 is a repetition of Intro and should be removed. Lines 319-323 belong to “Methods”.

We removed the sentence

The upper vertical stability maximum is associated with an increase of salinity near the top of the PWW and the lower stability maximum is associated with an increase in salinity between PWW and LHW.

and also the sentence

The new algorithm described in Sect. 2.2 was designed to provide estimates for the location of the cold halostad layer boundaries and the center, where the center is assumed to be the mean depth between the upper and the lower boundary.

However, we retained other sentences which do not merely repeat the introduction, but instead refer to and explain the profiles in Figure 5. We also retained the sentences which explain the occasional gaps in the green line in Figure 4b–d, although they indeed do repeat points previously explained in the methods section.

35. Line 332: Please direct the readers where exactly they can see the cold halostad near the coasts of Greenland in Fig. 8b.

Thank you very much. We now direct the readers to Figures 8a and b.

36. Lines 329-332: Fig 8c may benefit from showing Standard Errors – they may help address the problem stated in the text.

Yes, thank you very much. Instead of standard errors, we show the 95% confidence interval of the mean (roughly twice the standard error) in the revised version of Figure 8c. The relatively narrow confidence intervals suggest that the difference between August, September, and October and the other month cannot be explained by different spatial sampling with more points at the edge of the region in August, September, and October. We deleted this suggestion from Section 3.3. We also omitted the red line showing the fraction of grid points for which at least one observation was available in the respective month in the revised version of Figure 8c.

Response to reviewer comments by Marylou Athanase

Thank you very much for your very insightful second review and very constructive comments. We repeat your comments (using a dark blue font color) below. Our responses are given in black font.

This is my second round of reviews for this manuscript. In my first review of the original manuscript, my main concerns regarded (i) the reasoning being the choice of the ST criteria, (ii) the lack of direct evaluation of the methods, and (iii) improving the manuscript's readability. The authors have answered all my initial comments, and I find that the revised manuscript addresses well these three main concerns. The introduction and method description were greatly improved. The result section is now clearer and presented in a more linear way. I appreciate the addition of Figures 3, 5, and 7.

I still have a few remarks regarding editing and text clarifications, and one main comment which I trust the authors will be able to address. Overall, I believe the manuscript is close to being fit for publication, and would recommend acceptance after some minor revisions.

Main comment:

Since the choice of the DR criterion used for computing the ST criterion is, to some extent, somewhat arbitrary, it would be nice to add 1 or 2 sentences discussing this choice & how it should be optimized in the last section of the manuscript. You already touched on this topic by indicating that the ST criterion could be slightly changed to provide a better match with the DR criterion. This raises two questions:

- Should one aim for a match between both methods?
- If yes, are there particular reasons or limitations to why the adjustment of the ST criterion, following your own recommendations, could not be included in this manuscript as well? Adding an attempted "optimal ST criterion" for future users could strengthen your manuscript even more.

We think that one should not per se aim for a perfect match between the two methods. However, in the future it would probably be good to determine an ST threshold based on an empirical analysis of profiles, similar to how Bourgain and Gascard originally determined the DR threshold. We added the following sentences to the second paragraph of Sect. 4:

However, instead of simply aiming for a better match between the ST and the DR method, it may ultimately be more desirable to further fine tune the ST threshold based on an empirical analysis of profiles, similar to how Bourgain and Gascard (2011) determined the DR threshold. On the whole, estimating the ST threshold based on the DR threshold as we did provides fairly reasonable results, even without further fine tuning.

The second sentence is meant to discuss and defend our choice without downplaying the potential for improvement. Although we did not actually test using different ST thresholds, we do not expect major changes in the overall outcome, apart from probably a somewhat less deep halocline base in the Canadian Basin. In particular, we do not expect that moderate changes of the ST threshold would reduce the robustness of the ST method. Regarding new halocline formation, we may have to look for a different case to demonstrate that in principle the capping part is captured by the ST method. But again, we do not expect the overall conclusion to be affected by the exact choice of the threshold. In hindsight, we should have considered basing the ST threshold more on the empirical analysis of profiles and considered abandoning our idea of establishing a link with the well-established DR method.

Editing remarks:

L. 6 and 338: Could you clarify what is meant by “robust” here? Most likely is done in the core text, but if mentioned in the abstract it should be clear what the criteria are for readers.

In line 6, we omitted the sentence that explicitly stated our intention to develop a method that is more robust based on a suggestion by I. Polyakov. We retained the next sentence in which we connect “robust” with “few artifacts”. In line 338 we added “with few artifacts” in order to explain the meaning of “robust”.

L. 28-30: This is confusing: you first refer to the advection of shelf water onto more saline waters as a halocline formation mechanism. Yet in the following sentences, you state that this mechanism is supported by 2 other studies, but then cite the formation of halocline via ice melting on top of warm AW. Although there are similarities in these mechanisms, they are not exactly the same. In the first, the input of freshwater comes from the fresher shelf waters,

themselves fed by continental runoff and/or ice melt. In the latter, only direct ice melt on top of saltier waters is at play. Please clarify this statement.

Thank you very much. Based on a comments by both reviewers, we modified our discussion regarding the the interplay between convective homogenization and capping in the introduction of the manuscript. The revised section reads:

Based on data from the Oden 1991 cruise, Rudels et al. (1996) found that new halocline formation was initiated by the advection of relatively fresh shelf waters near the surface above denser and more saline water below, when the advection of the fresh water limited winter convection. Alkire et al. (2017) and Rudels et al. (2004) argued that convective homogenization and capping by fresh water due to sea ice melting in the inflow from the Fram Strait and the Barents Sea can transform AW into halocline water. Rudels et al. (2004) stressed that melting provides a precondition for sea ice formation and convective homogenization during the following winter.

We decided to omit the following sentence, which we deem less relevant in the light of our extended discussion on the roles of melt water:

Steele and Boyd (1998) argued that seasonal capping by melt water in summer may not be overly important for insulating the SML from relatively warm AW.

Throughout the manuscript, we now refer to the mechanisms that involve convective homogenization and capping as “convective homogenization and capping” instead of simply “capping”.

L. 40: This is again confusing. I understand what you mean, but calling the PWW both a part of the halocline and a halostad layer can appear contradictory. You could consider saying that the halocline in the Canada Basin is constituted of PHW, in which we distinguish a halocline layer formed by the PSW, which overlays a cold halostad formed by PWW, and below the PHW is found the strongly stratified LHW of Atlantic-origin. Adding a schematic figure of what these layers look like in a T-S profile could also help. You could point to the local stability maxima as well.

We omitted the reference to the statement by Zhong et al. (2019) that the PWW could be considered a type of cold halocline water. Regarding the local stability maxima, we refer to Supplement 1, which provides a schematic of the salinity and the stability profile and to Supplement 2 which shows profiles

based on observations. The salinity profile in the schematic is qualitatively similar not only to the profiles in Supplement 2, but also to the profiles shown in figure 2 of Shimada et al. (2005). The salinity and stability profiles in the schematic are also qualitatively similar to the corresponding profiles in Figure 5a and d except for the layer of Pacific Summer Water. They are also qualitatively similar to the corresponding profiles in Figure 5e and h except for the SML.

L. 50: typo “ist”

Thank you. We deleted the “t”, translating the German word “ist” (meaning “is”) into English.

L. 59: This sentence should rather be merged with line 52, here it is a little off-topic.

This stand-alone sentence is indeed awkward. However, we think that moving the sentence to line 52 would break the logic around line 52.

L. 67: “among others by others” typo

Corrected. Thank you.

L. 86-87: This sentence should be moved to the end of the previous paragraph (l. 59), as it results from emphasizing the importance of the halocline in the Arctic system.

We moved the sentence to the suggested paragraph, and linked it adding “Therefore,” at the beginning.

L.88: The manuscript outline is long and too detailed. Consider shortening this part, to no more than 1 sentence per section (1-2 lines) without detailing each sub-section. You might also not need to acknowledge your reviewers’ suggestions.

We shortened the section and cut the references to the reviews based in part also on a suggestion by I. Polyakov. The reviewers’ suggestions are still acknowledged in the acknowledgment section. But we did like the idea of citing

the reviews in the text, and had initially found numerous arguments to defend our choice of citing the reviews.

L. 148: “as demonstrated below” What does this refer to? This section? A figure?

We now refer to Supplements 1 and 2. Originally, we meant Fig. 5e and f.

Fig. 3: Nice figure. - tick labels are occasionally overlaying each other, consider fixing that - panel label and plot lines are occasionally overlaying each other, consider fixing that - if possible, would be great to have a profile of density as well.

We fixed most overlaps. Figures 3 and 5 of the revised manuscript include profiles of potential density.

L. 263-310. This section is interesting but quite dense. Consider breaking it down into several paragraphs, e.g., by adding a line break l. 271 (before “In addition”) and l. 283 (when transitioning to the Canada Basin).

Done. Thank you.

L. 275-277: Somewhat convoluted phrasing. In general, it is easier when sentences are straight to the point. In this case, you could just say that “the ST method also detects more frequent cases of halocline BD below 120 m compared to the DR method.”

Thank you very much. We changed

More frequent detections of halocline bases not only above 60 m but also below 120 m with the ST method compared to the DR method account for a slightly wider halocline base depth distribution in the Eurasian Basin in the ST method compared to the DR method (Fig. 7b).

to

The ST method also detects more frequent cases of halocline base depth below 120 m compared to the DR method (Fig. 7b).

L. 282: Any comments on this? You don’t make any use of Fig. 7c otherwise.

We now explicitly point out that the TD method “again” yields a greater halocline base depth compared to the other two methods, where the “again” refers to the base depth in the Eurasian Basin. This helps to highlight the contrast to the Canadian Basin, which is discussed starting with the next sentence.

L. 312-316: This is merely a suggestion, and you may choose or not to follow it: since you have already explained your concepts in section 2, you can consider removing the reminder of these concepts at the beginning of your subsections in section 3. Here, for example, lines 312-318 mostly repeat information provided in section 2. Since the paper is not overly long, you can however decide to maintain these reminders if you prefer to do so.

We removed some of the reminders (in part also based on a comment by I. Polyakov), but kept the ones which directly refer to the results in Fig. 5. We also removed a repetition from the method section in the same paragraph based on suggestion by I. Polyakov, but kept the repetitions that we use to explain the occasional gaps in the green line in Fig. 4.

L. 335: Redefine all acronyms in the summary section

Done.

L. 374: This is a bit colloquial (and rather pessimistic wording). Consider saying rather that e.g., “mismatch rates seem to be notably varying across ITPs tested. This suggests that further testing and refining are needed in order to account for regional and temporal variability of CHS characteristics”

Thank you very much. We reworded

while some other ITPs yielded almost perfect results and some other ITPs slightly worse results

to

albeit with detection rates varying across ITPs tested from almost perfect to a slightly higher mismatch rate

However, we retained our (more optimistic?) outlook. Although the method is not perfect, we do think that it may already be useful in its present form. In order to make this clearer, we modified the sentence:

This suggests that a stability-based method for CHS detection could be useful for future studies exploring variability and changes of the CHS in the Canada Basin.

to:

This suggests that the new stability-based method for CHS detection could be useful for future studies exploring variability and changes of the CHS in the Canada Basin.

L. 381: I would suggest rephrasing your very last sentence so that it highlights the potential of AI methods without discarding too harshly traditional methods (including your newly proposed one).

We removed the sentence

Given the various shortcomings of traditional threshold methods, AI-based methods could nevertheless be useful.

and instead speculate:

Rapid advances in AI may help to overcome these problems.

The original sentence was based on the (pessimistic) speculation that at least in the near future neither of the methods is likely to function perfectly, and on the (optimistic) speculation that in the meantime both methods may be useful in spite of their shortcomings.

Response to editor comment by Ilker Fer

When preparing your revision, could you also replace “Mai” with “May” (Fig 3e), and, if possible, make Figs7-8 50% or so taller?

Thank you very much. We replaced “Mai” with “May” in Fig. 3e, made the profile plots in Fig. 7 taller, and also enlarged and rearranged the panels in Fig. 8.

References

- Janzen, C., Larson, N., and Murphy, D.: Long-term accuracy, stability of Argo CTDs, Sea Technology, 2016.
- Spren, G., Kaleschke, L., and Heygster, G.: Sea ice remote sensing using AMSR-E 89-GHz channels, *J. Geophys. Res.*, 113, <https://doi.org/10.1029/2005jc003384>, 2008.
- Wong, A., Keeley, R., Carval, T., and Argo Data Management Team: Argo quality control manual for CTD and trajectory data, Tech. rep., <https://doi.org/doi.org/10.13155/33951>, 2023a.
- Wong, A. P. S., Gilson, J., and Cabanes, C.: Argo salinity: bias and uncertainty evaluation, *Earth Syst. Sci. Data*, 15, 383–393, <https://doi.org/10.5194/essd-15-383-2023>, 2023b.

Supplement of

**Technical note: Determining Arctic Ocean
halocline and cold halostad depths based
on vertical stability**

Enrico P. Metzner and Marc Salzmann

Correspondence to: Enrico Metzner (enrico.metzner@uni-leipzig.de)

- [supplement-title-page.pdf](#)
- [supplement1.pdf](#)
- [supplement2.pdf](#)
- [supplement3.pdf](#)
- [supplement4.pdf](#)
- [supplement5.pdf](#)
- [supplement6.pdf](#)

Supplement 1

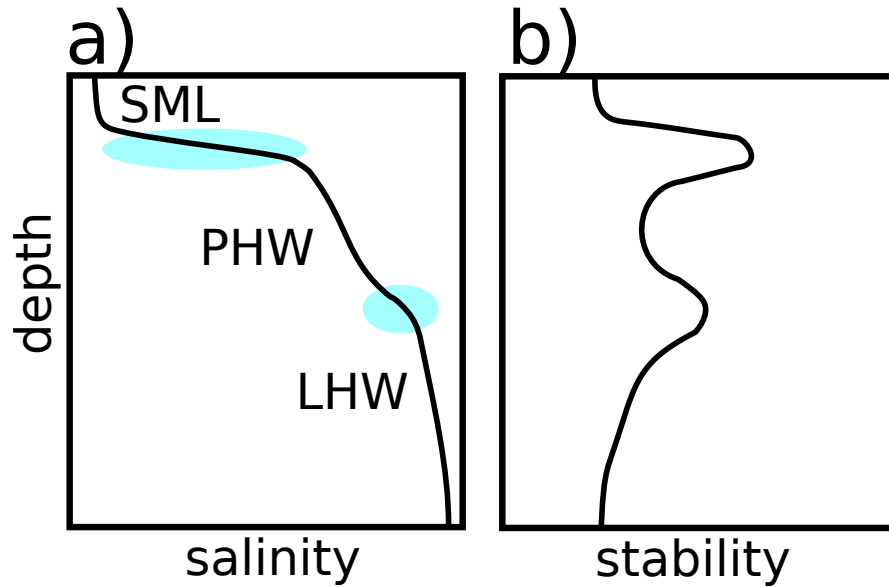


Figure S1. Schematic salinity (a) and stability (b) profile in the Canada Basin. Blue shadings in (a) indicate an increase in salinity below the surface mixed layer (SML) associated with the Pacific Halocline Water (PHW) and another increase associated with the Lower Halocline Water (LHW) below the PHW. These salinity gradients result in two distinct local stability maxima between the surface and the Atlantic Water below the LHW (b). The salinity profiles in (a) are similar to the ones in Shimada et al. (2005). Supplement 2 shows similar profiles for salinity and stability from ITP-41 in the Canada Basin and also includes temperature profiles.

Supplement 2

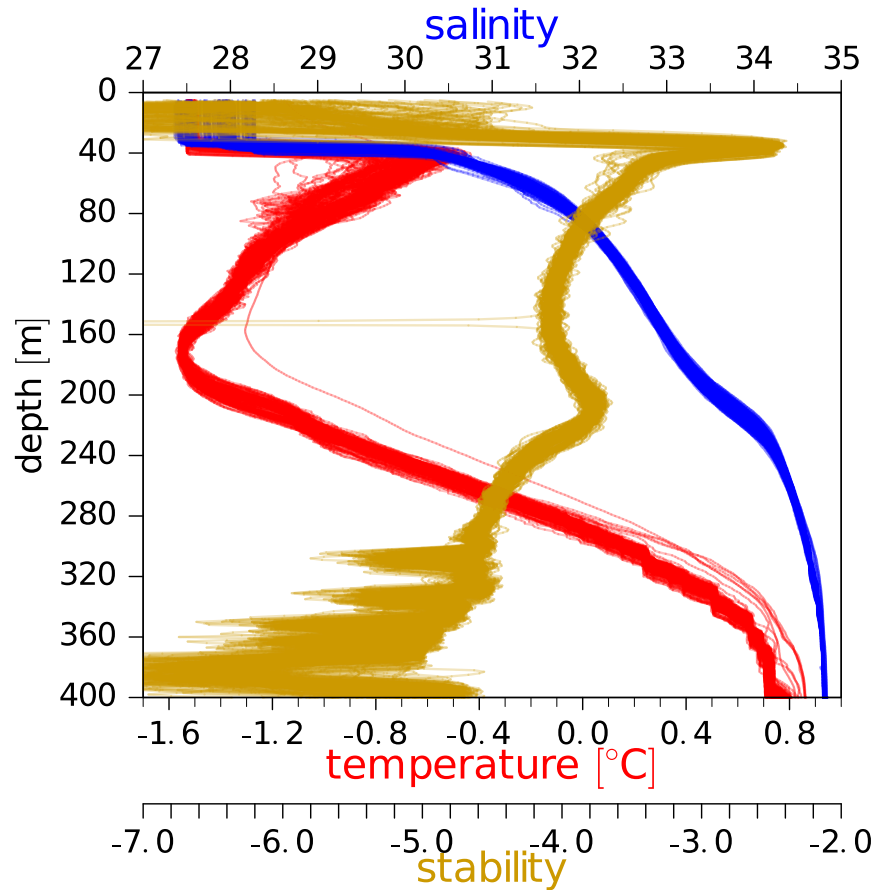


Figure S2. Profiles of salinity (blue), temperature (red), and stability (brown) from ITP-41 Level III data for days from 16 Feb 2011 to 27 May 2011 (Krishfield et al., 2008; Toole et al., 2011). Compare also schematic in Supplement 1. Salinity is in the practical salinity scale. Stability (L , unitless) was computed as described in Sect. 2.1.3. Below 280 m, thermohaline staircases are found in the Atlantic Water.

Supplement 3

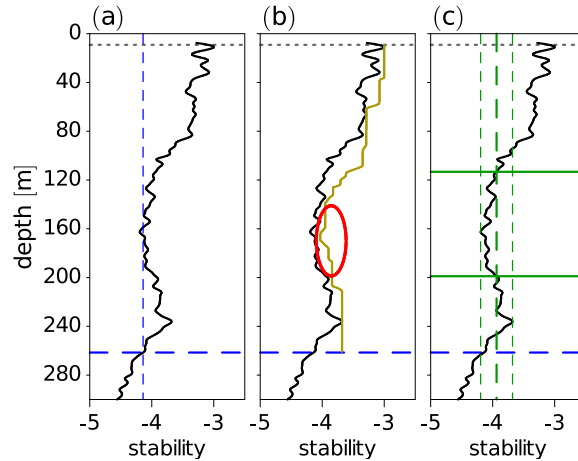


Figure S3. Example: determining the CHS boundaries and center depth (see Sect. 2.2) based on the stability profile for ITP-33 on 6 September 2010. Corresponding temperature and salinity profiles are shown in Fig. 5f. Please refer to the text below for an explanation of the figure.

First, the base of the halocline is estimated using the stability algorithm as described in Sect. 2.1.3 (a). The thin vertical blue dashed line in (a) indicates the stability threshold for estimating the halocline base (searching upward). The horizontal thick blue dashed line indicates the halocline base and the dotted gray line the SML base (computed as described in Sect. 2.3). Then, between the SML base and the halocline base, a moving maximum is computed for the stability as described in Sect. 2.2 (brown line in (b)). The first condition for detecting a CHS is met if a minimum is found above the halocline base between two stability maxima based on the moving maximum profile (red circle). This implies that the distance between the deeper stability maximum and the first upper occurrence of that same stability value must be at least 50 m. An additional condition for identifying the CHS is that the difference of the stability L between the lower stability maximum and the local minimum (i.e. the “amplitude” of the minimum) in the CHS is at least 0.2. If these conditions are met, we compute the mean (thick dashed vertical green line in (c)) of the stability minimum and the deeper stability maximum (thin dashed vertical green lines in (c)). This stability value is used as a threshold to identify the upper and the lower bound of the CHS (horizontal solid green lines in (c)). The center depth of the CHS is defined as the mean depth between the upper and the lower bound (not shown here). The conditions regarding the minimum vertical extent and the amplitude of the stability minimum described above help to minimize the number of false CHS detections.

Supplement 4

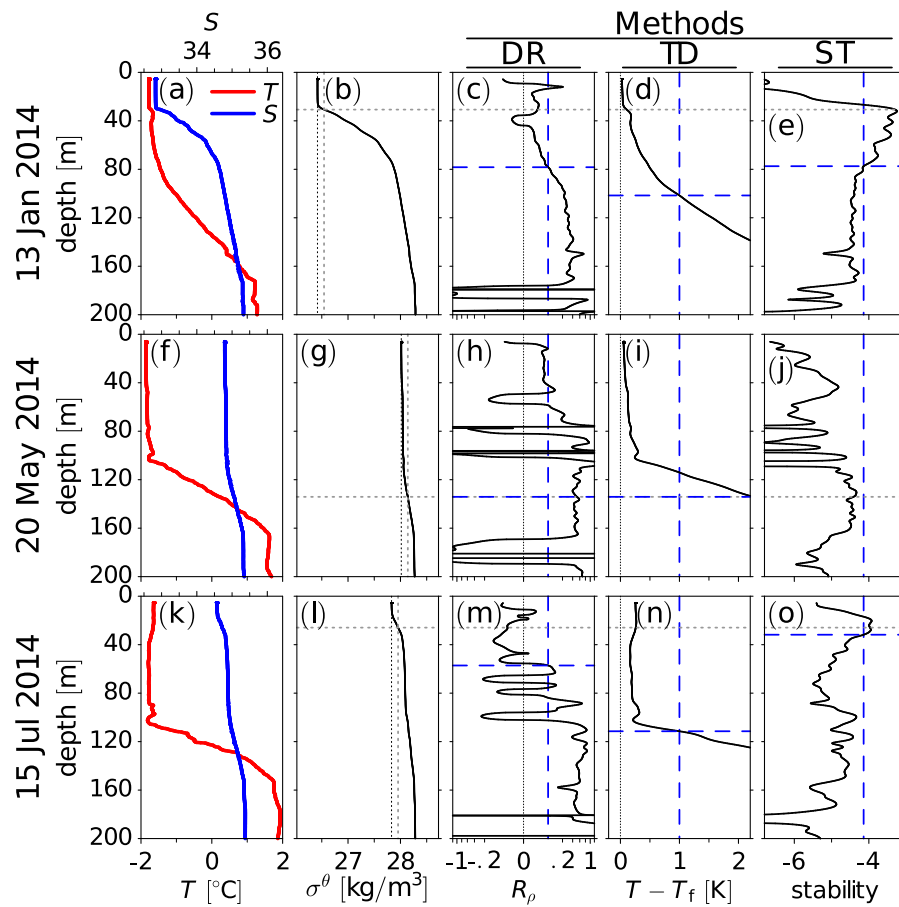


Figure S4. As Fig. 3 but based on Level I data and using the International Thermodynamic Equation of Seawater – 2010 (TEOS2010, McDougall et al., 2010) to compute potential density, potential temperature, and potential freezing temperature instead of Gill (1982).

Supplement 5

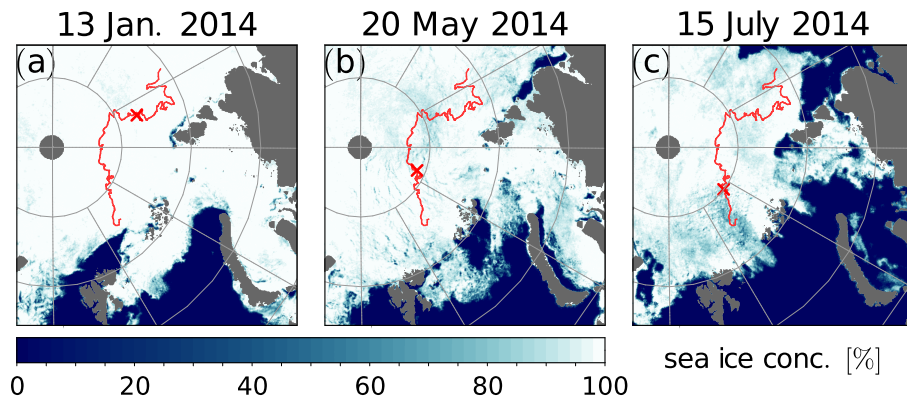


Figure S5. ITP-74 location of measurements (indicated by small red crosses along the tracks) and sea ice concentration (area fraction) from Spreen et al. (2008) for the profiles shown in Figure 3. Sea ice data was obtained from <https://www.meereisportal.de> (Grosfeld et al., 2016).

Technical note: Determining Arctic Ocean halocline and cold halostad depths based on vertical stability

Enrico P. Metzner¹ and Marc Salzmann¹

¹Institute for Meteorology, Universität Leipzig, Leipzig, Germany,

Correspondence: Enrico P. Metzner (enrico.metzner@uni-leipzig.de)

Abstract. The Arctic Ocean halocline separates the cold surface mixed layer ^{1.P}(SML) from the underlying warm Atlantic Water (AW), and thus provides a precondition for sea ice formation. Here, we introduce a new method in which the halocline base depth is diagnosed from vertical stability and compare it to two existing methods. ^{1.P}We also propose a novel method for detecting the cold halostad, which is formed by Pacific Winter Water in the Canada Basin or by melt water off the eastern coast of Greenland and also Svalbard. Our main motivation for diagnosing the halocline base depth ^{1.P}depending based on vertical stability was that vertical stability is closely related to vertical mixing and heat exchange^{1.P}. Unlike parameters previously used to detect the halocline base, vertical stability is a crucial parameter for determining whether the halocline can prevent vertical heat exchange and protect, and thus also to the role of the halocline in preventing vertical heat exchange and thereby protecting sea ice from warm AW. ^{M.A and 1.P}The second goal was to provide a particularly robust method. When applied to measurements from ice-tethered profilers, ships, and moorings, the new method for estimating the halocline base depth provides robust results with few artifacts. ^{1.P}Analyzing a case in which water previously homogenized by winter convection was capped by fresh water at the surface suggests that the new method captured the beginning of new halocline formation in the Eurasian Basin. Comparatively large differences between the methods for detecting the halocline base depth were found in warm AW inflow regions for which climate models predict ^{1.P}halocline thinning and increased net surface energy fluxes from the ocean to the atmosphere^{1.P}, suggesting that these regions may be particularly sensitive to a halocline retreat. ^{1.P}Analyzing a case in which water previously homogenized by winter convection was capped by fresh water at the surface suggests that the new method captured the beginning of new halocline formation in the Eurasian Basin. ^{1.P}We also propose a novel method for detecting the cold halostad (CHS), which is formed by Pacific Winter Water (PWW) in the Canada Basin or by melt water off the eastern coast of Greenland and also Svalbard.

20 1 Introduction

The Arctic Ocean outside the main Atlantic warm water inflow ^{1.P}regions and the shallow marginal shelf seas is usually stratified into a cold and fresh surface mixed layer (SML), which is from ~5 to >100 m thick, depending on region and season (Peralta-Ferriz and Woodgate, 2015), a halocline below the SML with a base depth ~40 to >200 m (Fig. 4 of Polyakov et al., 2018), a layer of warm and saline Atlantic Water (AW) below the halocline centered near 300 to 500 m in the Eurasian Basin and somewhat deeper in the Canada Basin (Aagaard et al., 1981; Macdonald et al., 2015), and deep water below. Convection

in the SML is driven by surface cooling and brine release during sea ice formation, with maximum SML depth in winter. River inflow and precipitation act as sources of fresh water. Below the SML, salinity increases in the halocline. Within the halocline, one can distinguish between the cold halocline layer (CHL) in the Eurasian Basin, the Pacific Halocline Waters (PHW, modified Pacific Water which originally entered the western Arctic via the Bering Strait) in the Amerasian Basin, and the lower halocline waters (LHW, water of Atlantic origin which is less modified compared to CHL water) (e.g. Alkire et al., 2017; Polyakov et al., 2018; Anderson et al., 2013). In the CHL, the temperature remains close to the freezing point. Several processes have been suggested as contributors to LHW and CHL formation. Based on data from the *Oden* 1991 cruise, Rudels et al. (1996) found that new halocline formation was initiated by the advection of relatively fresh shelf waters near the surface above denser and more saline water below, when the advection of the fresh water limited winter convection. ^{M.A and I.P}Support for the importance such a capping process was provided by Alkire et al. (2017) and Rudels et al. (2004)^{M.A and I.P}. They argued that ^{M.A and I.P}convective homogenization and capping by fresh water due to sea ice melting in the inflow from the Fram Strait and the Barents Sea can transform AW into halocline water. ^{M.A and I.P}Rudels et al. (2004) stressed that melting provides a precondition for sea ice formation and convective homogenization during the following winter. Another process which has been widely discussed, and which is thought to be especially important for the PHW is the advection of dense and saline shelf waters (where salinity increases due to brine release during sea ice formation especially in winter) below the SML (Aagaard et al., 1981; Jones and Anderson, 1986; Rudels et al., 2004). While halocline formation via ^{I.P}convective homogenization and capping does not require dense shelf waters, ^{I.P}convective homogenization and capping can also occur after (i.e. in addition to) the advection of dense shelf water (Steele and Boyd, 1998; Rudels et al., 2004). ^{M.A and I.P}Steele and Boyd (1998) argued that seasonal capping by melt water in summer may not be overly important for insulating the SML from relatively warm AW. The PHW in the Canada Basin originates from Pacific Water inflow, which is modified on the Chukchi Sea Shelf, ^{I.P}whilebut the LHW is of Atlantic origin ^{I.P}not only in the Eurasian Basin but also in the Canada Basin (e.g. Anderson et al., 2013). Because of seasonal modifications on the Chukchi Sea Shelf, the PHW in the Canada Basin can be further subdivided into Pacific Winter Water (PWW) and less saline and warmer Pacific Summer Water (PSW) (e.g. Timmermans et al., 2014). ^{M.A}CThe PWW could be referred to as a type of cold halocline water (Zhong et al., 2019), although compared to the CHL in the Eurasian Basin, in the PWW, the salinity is lower and the salinity gradient is smaller. This is why Shimada et al. (2005) called the layer which is formed by PWW a cold halostad (CHS). ^{I.P}Similarly, interaction between glacial melt water and Arctic water north east of Greenland forms an intermediate low salinity layer with small salinity gradient which is also called a cold halostad (Dmitrenko et al., 2017). Below, we argue that ^{I.P}an increase in salinity associated with the PHW and another increase associated with the LHW results in two distinct local stability maxima between the surface and the LHW (compare also schematic in Supplement 1 and profiles in Supplement 2)a lower salinity and a smaller salinity gradient in the CHS compared to the LHW below results in two distinct local stability maxima between the base of the LHW and the SML base: The upper stability maximum is associated with an increase of salinity in the upper PWW. The lower stability maximum is associated with another increase of salinity in the LHW. The lower one of these two stability maxima is absent in the presence of a CHL in the Eurasian Basin (except in regions off the eastern coast of Greenland and also Svalbard^{I.P}where melt water also forms a CHS). ^{I.P}This allows us to

60 identify the CHS. ^{I.P}North east of Greenland glacial melt water forms an intermediate low salinity layer with small salinity gradient which is also called a cold halostad (Dmitrenko et al., 2017).

Because density is more influenced by salinity than temperature if the temperature is low (Aagaard et al., 1981; Roquet et al., 2022) a configuration with warm AW underlying colder halocline water is ^{M.A and I.P} stable. The presence of a (cold) halocline thus insulates the SML from direct contact with the warm AW and protects sea ice from the warm AW (Aagaard et al., 1981; 65 Lind et al., 2016; Polyakov et al., 2017, 2020). Conversely, a retreat of the CHL in the Eurasian Basin leads to increased vertical mixing as observed and described by Steele and Boyd (1998); Björk et al. (2002); Polyakov et al. (2017). Retreating sea ice, increased surface heat flux and the retreat of the halocline have been called atlantification of the Eurasian Basin (Polyakov et al., 2017). Future climate model projections for a high emission scenario also showed very large temperature gradients directly below the surface mixed layer more frequently, especially during the cold season. The associated heating of the SML 70 in combination with sea ice loss resulted in further increased annual mean upward net surface energy fluxes outside the Central Arctic along the main warm water inflow pathways (Metzner et al., 2020). ^{M.A} Therefore, consistent and robust descriptions of the halocline and cold halostad layer boundaries are important to understand the evolution of the structure of the upper Arctic Ocean in the past and the future. While the halocline generally protects sea ice, PSW can be warm enough to participate in sea ice melting ^{I.P} (e.g. Shimada et al., 2006; Timmermans et al., 2014) (e.g. Timmermans et al., 2014).

75 Several methods have been proposed for identifying the halocline based on observations. Steele et al. (1995) identified cold halocline water based on conditions for salinity ($34 < S < 34.5$ in the practical salinity scale) and temperature ($T < -0.5^{\circ}\text{C}$). Rudels et al. (1996) defined the boundaries of the CHL by using the 34.3 isohaline. Bourgain and Gascard (2011) used a density ratio threshold to define the base of the halocline. The density ratio is the ratio of temperature and salinity contributions to the vertical stability. A large density ratio implies that the vertical stratification is dominated by temperature and a small density 80 ratio implies that stratification is dominated by salinity. The density ratio threshold suggested by Bourgain and Gascard (2011) assumes that oceanic layers above the halocline base are almost entirely salt-stratified with temperature contributing less than 5% to the total stratification (Polyakov et al., 2018). This density ratio method was adopted among others ^{M.A} ~~by others~~ by Polyakov et al. (2017, 2018) and Metzner et al. (2020). Using tracer observations in the western Eurasian Basin, Bertosio et al. (2020) found the base of the LHW to be located at a density of $1027.85 \text{ kg m}^{-3}$. Analyzing salinity and temperature 85 observations from the Makarov Basin and along the East Siberian continental slope, Bertosio et al. (2022) again defined the base of the halocline using a density threshold and compared the results obtained with this definition to those obtained with other definitions from the literature. A fairly simple and robust method for computing the CHL base depth was proposed by Metzner et al. (2020). In this method, the base of the CHL is determined by a temperature difference of 1°C between water potential temperature and its freezing temperature. This temperature difference method is very sensitive to warming from 90 below, while the density-ratio method of Bourgain and Gascard (2011) is very sensitive to the salinity profile. One drawback of the temperature difference method is a potential dependence of the optimal threshold value on region (Metzner et al., 2020). Polyakov et al. (2018) proposed an indicator of the potential of the Arctic halocline to prevent vertical mixing based on available potential energy, adapting the density ratio threshold of Bourgain and Gascard (2011) to identify the halocline base.

Here, we propose a new method to identify the halocline base using a vertical stability threshold and compare it to two existing methods using measurements from ice-tethered profilers, ships, and moorings. Our main objective was to devise a method that uses a threshold value of a variable which is closely related to the role of the halocline in insulating the SML from the warm AW. The choice of a vertical stability threshold was motivated by the argument that vertical stability is more directly related to vertical mixing than either density, temperature, or the density ratio. Our second goal was to devise a particularly robust method to detect the halocline base. Based on the argument that the presence of PWW forming a CHS on top of LHW creates a stability profile with two distinct local stability maxima, we also propose a method for estimating the boundaries and the center of the CHS. ^{M.A.} Consistent and robust descriptions of the halocline and cold halostad layer boundaries are important to understand the evolution of the structure of the upper Arctic Ocean in the past and the future.

In the next section, we ^{M.A.} first describe methods to determine the halocline base depth ^{M.A.}, a starting with two existing methods which are used for comparison, i.e. the density ratio (DR) method by Bourgain and Gascard (2011), and the temperature difference (TD) method by Metzner et al. (2020). We then introduce our new stability (ST) method for determining the halocline base depth. In Section 2.2, we propose a new method for estimating the CHS upper and lower boundaries and the CHS center, ^{M.A.} and which is based on vertical stability as well. In Section 2.3, we describe a method for estimating the SML base depth because the downward search for the DR and the TD threshold starts at the SML base and because the top of the halocline is assumed to coincide with the SML base. In Sect. 2.4, we introduce observational datasets used for comparison and testing. In Sect. 3, we compare the new ^{M.A.} stability ST method for determining the halocline base depth to ^{M.A.} two existing methods and test the new method for determining the CHS depth and extent. ^{M.A and I.P.} We first compare the methods to determine the halocline base using case studies and investigate whether the ST method captures the beginning of new halocline formation based on a suggestion in a reviewer comment on the original submission by Polyakov (2023) in Sect. 3.1. We then use maps and basin-wise statistics (based on a suggestion in a reviewer comment by Athanase, 2023) in Sect. 3.2. The performance of the CHS algorithm is discussed in Sect. 3.3. The results are summarized and discussed Sect. 4.

2 Methods and Data

2.1 Methods for estimating the halocline base depth

2.1.1 Density ratio (DR) method

In ^{I.P.} the Arctica halocline, the density gradient due to temperature ^{I.P.} is must be small compared to the density gradient due to salinity by definition (Bourgain and Gascard, 2011). The density ratio (DR) method by Bourgain and Gascard (2011) therefore identifies the halocline base by the requirement that the ratio R_ρ between the density gradient due to temperature and the density gradient due to salinity must remain below a certain threshold. The density ratio is defined as $R_\rho = (\alpha \nabla_z \theta) / (\beta \nabla_z S)$ with potential temperature θ in °C, salinity S in the practical salinity scale and depth z in m. $\alpha = -\rho^{-1}(\partial\rho/\partial\theta)$ and $\beta = \rho^{-1}(\partial\rho/\partial S)$ are the thermal expansion coefficient and the haline contraction coefficient, respectively. Bourgain and Gascard (2011) empirically estimated that searching downward for the depth, in which R_ρ exceeds 0.05, provides a reasonable estimate

for the base of the halocline. The search starts at the base of the SML (here determined as described in Sect. 2.3 below), which is defined to be the top of the halocline layer. If the density ratio threshold is exceeded already directly at the base of the SML, then no halocline was detected for the corresponding profile. Such profiles are excluded when computing statistics of halocline base depths. Similarly to Bourgain and Gascard (2011), we smoothed the S and θ prior to computing the density ratio as explained in Sect. 2.4.

2.1.2 Temperature difference (TD) method

The temperature difference (TD) method (Metzner et al., 2020) uses the difference ΔT between the ocean temperature T and the sea water freezing temperature $T_f T_{freeze}$ to estimate the cold halocline base depth. The freezing temperature was calculated from Gill (1982). Searching downward, starting at the SML base, the base of the halocline was calculated as the depth, in which ΔT first exceeds 1 K. This threshold was estimated to be high enough, that the "cold" core of the cold halocline layer is detectable, and low enough to separate the CHL from the AW with core temperature approximately 1.5°C to 3°C ($T_f \approx -2^\circ\text{C}$ leads to $\Delta T \approx 3.5^\circ\text{C}$ to 5°C at the core). In cases in which the temperature threshold was first exceeded in a depth shallower than 80 m, the search was continued 0.5 m below this depth. If the temperature threshold was exceeded already at the SML base, no halocline was detected. The algorithm was applied to smoothed temperature data (see Sect. 2.4).

2.1.3 Stability (ST) method

The new stability (ST) method prescribes a threshold for the local vertical stability in order to estimate the halocline base depth. Vertical stability is more closely related to vertical mixing than either the density ratio or the temperature difference. ^{1,P}However, while vertical stability is closely related to vertical heat exchange and to the role of the halocline for protecting sea ice, the density ratio is more directly related to the original definition of a halocline.

Because the search direction was found to affect the robustness of the method, and because stability is decreasing with depth between the AW and the core of the halocline, we search upward instead of downward for the stability threshold. The stability was computed from $L = \log_{10}(N^2)$, where $N = \sqrt{-(g/\rho)(\partial\rho/\partial z)}$ is the Brunt-Väisälä-frequency (with density computed from pressure, smoothed S , and θ as described below). The stability threshold was approximated based on the density ratio threshold $R_\rho = 0.05$ assuming an approximately constant salinity gradient near the halocline base in the LHW. It was derived starting from the following relationship:

$$\rho^{-1}\nabla_z\rho = \beta\nabla_z S - \alpha\nabla_z\theta = \beta\nabla_z S(1 - R_\rho) \quad (1)$$

With stable $\beta = (7.82 \pm 0.03) \cdot 10^{-4}$ over a wide range of temperature, salinity and pressure values ($-1.2 \dots 2.0^\circ\text{C}$, $32 \dots 37$, $50 \dots 350$ dbar) and the salinity gradient in m^{-1} :

$$L = \log_{10}(-\nabla_z S) - 2.137 \pm 0.002 \quad (2)$$

Expecting the salinity gradient to be around 0.01 m^{-1} near the base of the halocline, the resulting stability threshold should be $L \approx -4.14$.

This threshold is searched from 600 m or at the lowest point (at least 500 m deep outside the shallower regions according to the conditions for including profiles in the analyses described below in Sect. 2.4) to the surface, as no CHL base was observed deeper than that. Seldom, the first estimate is in warm AW at $T > 0^\circ\text{C}$. In such cases, a second search for the stability threshold is started slightly above. If the stability threshold is never exceeded or only exceeded where $T > 0^\circ\text{C}$ in a given profile, then no halocline base was detected for this profile.

2.2 Cold halostad (CHS) boundary and center estimates

A CHS is formed by PWW in the Canada Basin and also by melt water off the eastern coast of Greenland and Svalbard. Compared to the CHL in the Eurasian Basin, a CHS is characterized by a smaller salinity gradient because of the different water origins. ^{M.A and I.P}As demonstrated below in Sect. 3.3, ~~t~~his leads to one local stability maximum ~~above~~at the ~~top of~~ the CHS (at the transition between SML ~~or PSW~~ and PHWPWW and a second stability maximum associated with the transition between PHWCHS and ~~the~~ LHW^{M.A and I.P} (compare also Supplement 1 and 2). The stability minimum between these two local stability maxima is associated to the CHS. Therefore, as a first condition for identifying a CHS, we require that more than one local stability maximum must be present between the base of the SML and the base of the hal^{I.P}ocline as identified by the ST algorithm described above. Because the stability profiles computed from temperature and salinity observations contain small scale fluctuations even after smoothing the S and θ data that is used for computing density as described below, we identify local maxima by first computing a “moving” stability maximum for a 50 m vertical box surrounding each observation. This moving stability maximum is computed from $L_m(z) = \max(L(z'))$ for $|z' - z| < 25$ m), where z is depth ^{I.P}Please refer to Supplement 3 for an example illustrating the entire procedure for estimating the CHS boundaries and center depth. The moving maximum operation is illustrated by an example in Fig S3b in Supplement 3. This moving maximum operation was defined in analogy to a moving average. The result is a profile of stability maxima $L_m(z)$ with few local maxima. We then compute the mean of the ^{I.P}deeperlower stability maximum, which is associated with the transition between PHWCHS and LHW, and the stability minimum between the upper and the lower stability maximum, which is associated with the CHS ^{I.P}based on the original smoothed stability profile (Supplement 3). This value is used as a threshold to define the upper and the lower boundary of the CHS. The depth of the center of the CHS is defined as the mean of the upper and lower boundary of the CHS. A CHS will only be recognized by the algorithm if the vertical distance between the deeper stability maximum and the first upper occurrence of that same stability value is at least 50 m, and the difference of L between the lower stability maximum and the local minimum in the CHS is at least 0.2. With this definition, we never identified more than a single CHS per profile.

2.3 SML depth estimate

The SML depth was estimated by a change in potential density of 0.125 kg m^{-3} at the surface as in Polyakov et al. (2017). In cases, in which a CHL is detected, the depth of the SML corresponds to the top of the CHL. Potential density was computed from smoothed S and θ . ^{M.A.}The smoothing was performed using a Gaussian filter as described in the next section.

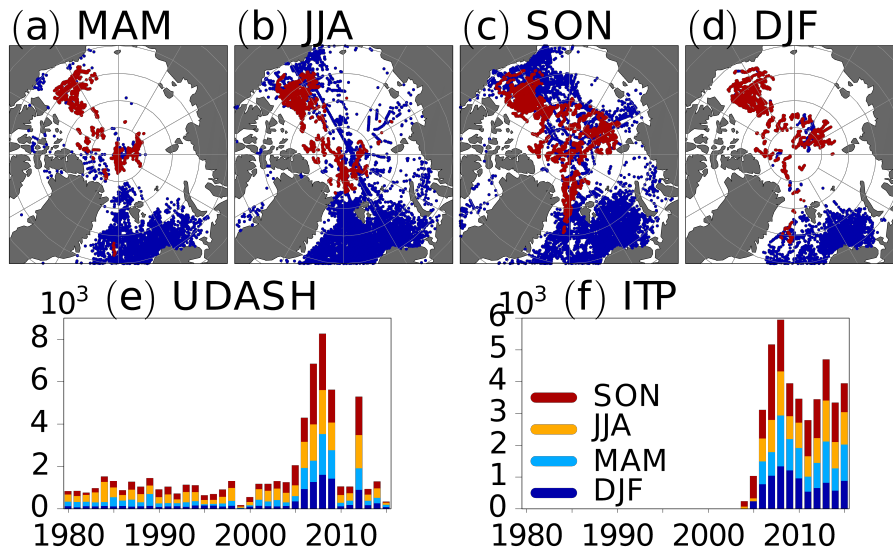


Figure 1. Locations of observations for each season (starting with MAM for March, April, and May) with blue dots for UDASH profiles and red dots for ITP profiles (a–d). Temporal coverage for UDASH (e) and ITP (f) observations.

2.4 Data and preprocessing

Temperature and salinity observations were taken from the ice tethered profiler (ITP) project (Krishfield et al., 2008; Toole et al., 2011) and the Unified Database for Arctic and Subarctic Hydrography (UDASH, Behrendt et al., 2018). The ITPs measured temperature, salinity, and pressure twice a day while drifting with the ice floe they were tethered to. Data processing for the ITP data is described by Krishfield et al. (<http://www.whoi.edu/filesserver.do?id=35803&pt=2&p=41486>). Here, we used processed ITP Level III data. Producing Level III data included removal of corrupted data, corrections for the sensor response behavior, calibrations, and final screening of spurious outliers. ITPs deployed in the Arctic Ocean before 2018 were included here. The vertical resolution for ITP level III data is 1 ± 0.1 dbar. The accuracy of the sensors used for the ITP observations ^{1.P}has been cited as 0.002 °C for temperature and 0.002 for salinity (Polyakov et al., 2017)^{1.P} in agreement with an assessment by the manufacturer (Janzen et al., 2016). For temperature, this accuracy range is supported by Wong et al. (2023a). For salinity, larger biases can arise due to sensor shift on longer time scales, depending on the manufacturing date of the sensor (Wong et al., 2023b). The UDASH data set contains data from ships, ice-tethered profilers, profiling floats and other platforms (Behrendt et al., 2018). Only profiles, for which both temperature and salinity were available, were analyzed here. Furthermore, only profiles with a vertical resolution finer than 2.5 dbar in the upper 300 m and a vertical resolution finer than 5 dbar elsewhere were used. We also required that the deepest point in a profile must reach at least 500 m or 90% of the basin depth. This choice addresses the issue of potential sampling biases due to limited vertical extent of the observed profiles. Regions shallower than 100 m were always excluded from the analysis. Bathymetry data was taken from the General Bathymetric Chart of the Oceans (GEBCO) dataset (GEBCO Bathymetric Compilation Group 2021, 2021). This filtering left a total of 43715 ITP and

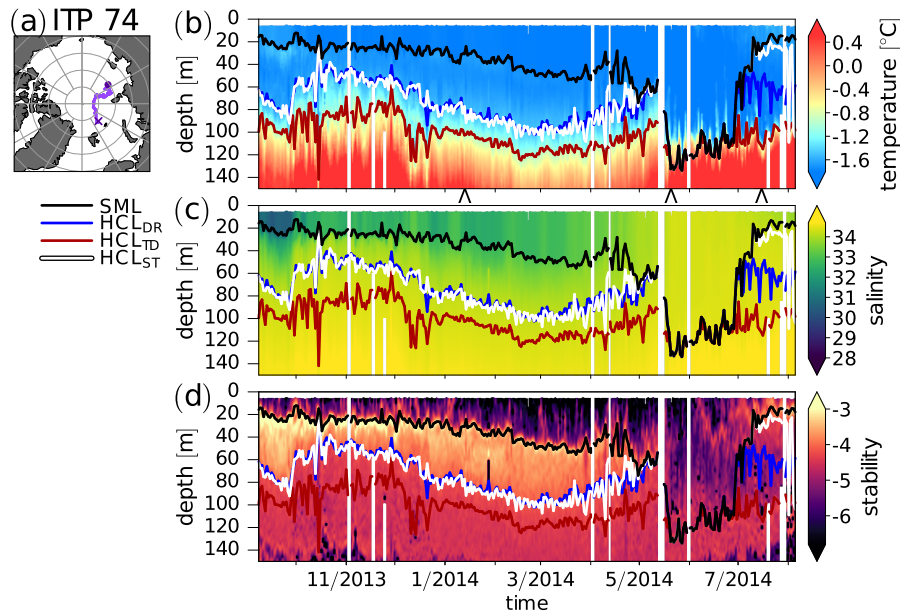


Figure 2. ITP-74 location of measurements (a) and time series of temperature (b), salinity ^{IP}(in the practical salinity scale) (c), and vertical stability ^{IP}(L , unitless, see Sect. 2.1.3) (d). The circle and the cross in (a) mark the beginning and the end of the ITP-74 track, respectively. The colored lines in (b–d) are the base of the SML (black) and the halocline (HCL) base depths derived by the DR method (blue), the TD method (red) and the ST method (white). ^{IP}Salinity is given in the practical salinity scale. Individual profiles at the location of the wedge symbols (\wedge) below the x-axis in (b) are shown in Fig. 3. Profiles that started below 15 m were excluded (only) in this figure (but nowhere else), because this increased readability by reducing the effect of noise in determining the SML base without affecting the overall result.

62012 UDASH profiles. Figure- 1 provides an overview of the spatio-temporal coverage of the data. Most measurements are concentrated in the Barents Sea and only few were taken in the Central Arctic during winter. For the East Siberian Sea and the interior of the Laptev Sea, no data was available for winter and spring. Salinity was given in the practical salinity scale.

210 Depth was computed from pressure using the hydrostatic equation. Density was computed based on salinity, temperature, and pressure. In order to reduce noise, S , T , and/or θ were smoothed using a standard one-dimensional Gaussian filter (convolution with a Gaussian function, e.g. Deng and Cahill, 1993) with a standard deviation of 2 dbar and a truncation at ± 10 dbar. When using thresholds to estimate the SML or CHL base depth, variables were linearly interpolated between two adjacent depths. Consequently, the SML or CHL base can be located between two vertical observation points and the SML and CHL base depths do not necessarily have to coincide with the depths of the observations.

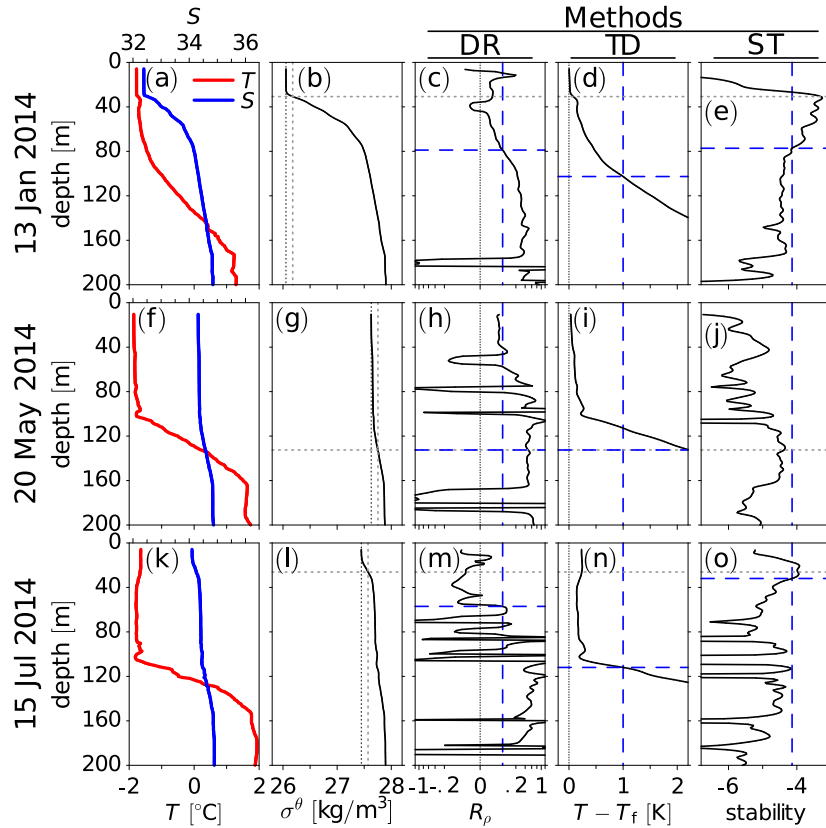


Figure 3. Please note: Added profiles of potential density anomaly and fixed overlapping labels. Temperature T and salinity $S^{\text{M.A and I.P}}$ (a, f, k), potential density anomaly $\sigma^\theta = \rho^\theta - 1000 \text{ kg m}^{-3}$, where ρ^θ is potential density (b, g, l), density ratio R_ρ (please note the cubic scaling of the x-axis) (c, h, m), temperature difference $T - T_f$, where T_f is the freezing temperature (d, i, n), and stability L (e, j, o) from ITP-74 before winter convection on 13 January 2014 (a–e)–(a–d), during winter convection on 20 May 2014 (f–j)–(e–h) and after winter convection on 15 July 2014 (k–o)–(i–l). ^{M.A and I.P}Vertical dotted lines in b, g, l indicate the surface density anomaly and the threshold for determining the SML base (i.e. surface density plus 0.125 kg m^{-3}). Horizontal dotted lines indicate the SML base. Vertical dashed lines indicated threshold values for determining the halocline base. Horizontal dashed lines indicate the halocline base determined by the three different methods. ^{M.A and I.P}Dotted lines indicate the SML base. ^{I.P}Dashed lines overlying dotted lines indicate that a threshold for identifying the halocline base was exceeded at the SML base.

215 3 Results

3.1 Comparison of methods for deriving halocline base depth using case studies

Figure 2 compares three different methods for determining the halocline base depth for ITP-74. Starting from the Laptev Sea in September 2013, ITP-74 drifted across the Central Arctic, almost reaching the East Greenland Sea (Fig. 2a). Until May 2014, Fig. 2b–d shows evidence of a well-defined and stably stratified CHL below the SML. The vertical stratification observed

220 by ITP-74 prior to May 2014 and the performance of the three methods for determining the halocline base depth are further analyzed in an individual profile from this period in Fig. 3. ^{I.P}[Supplement 4 shows a corresponding figure based on Level I data instead of the more processed Level III data and equations from McDougall et al. \(2010\) instead of Gill \(1982\).](#) [Supplement 5 shows the locations of the profiles analyzed in Fig. 3 together with maps of sea ice concentration based on Spreen et al. \(2008\).](#)

Individual profiles of salinity and temperature for 13 January 2014 in Fig. 3a show the base of the SML at about ~30 m.
225 Between the SML base and ~80 m a strong salinity gradient and temperatures close to the freezing point indicate a well defined CHL, which is ~60 m thick. Between the CHL and the AW, temperature and salinity increase in the LHW. Below ~170 m warm and saline AW is found (please note ^{I.P}~~the kink in the temperature and salinity profiles~~ that at ~170 m^{I.P}, ~~the temperature and salinity slopes~~ in Fig. 3a^{I.P} ~~both change~~). ^{M.A and I.P}[The potential density anomaly used to compute the SML base is shown in Fig.3b.](#) Figs [3c-e](#) ~~b-d~~ show the density ratio, the temperature difference, and the stability for the observations
230 on 13 January 2014^{I.P}. ~~T together with the~~ threshold values used to identify the halocline base with the DR, the TD, and the ST method ^{I.P}~~are also shown~~. For the profile observed on 13 January 2014, the DR method (Fig. [3cb](#)) and the ST method (Fig. [3e d](#)) identify the CHL base, while the TD method ^{I.P}~~(Fig. 3d)~~ places the halocline base in the LHW, somewhere between CHL and AW^{I.P} (Fig. [3c](#)). The stability profile in Fig. [3de](#) yields distinctly different stabilities for the SML, the CHL, the LHW, and the AW.

235 In May 2014, the SML deepens and the CHL disappears (Figure 2), as previously noted by Polyakov et al. (2017). During this convection event, neither of the three methods identified a halocline. Figs [3h-je-h](#) show profiles for 20 May 2014 after the onset of convection. On this date, the threshold for identifying the halocline base was already exceeded at the SML base for the DR and the TD method (Fig. [3hf](#) and [ig](#)), while the threshold was not reached for the ST method (Fig. [3jh](#)). ^{I.P}~~In~~After July, the situation becomes particularly interesting. The stability at about 80 m depth remains low, pointing to the residual of a mixed layer well below the diagnosed SML base (Figure 2). Fig. [3ki](#) for 15 July 2014 (after convection) also shows freshening and warming near the surface. This indicates that relatively fresh melt or/and shelf water may have been advected above a colder and saline layer, which had previously been homogenized by winter convection. The freshening near the surface leads to a salinity gradient below, and also a stability maximum, which is captured by the ST method (Fig. [3oh](#)). This appears to be consistent with the ^{I.P}[convective homogenization and capping](#) mechanism for halocline formation described by Rudels et al.
240 (1996). ^{I.P}~~As stated above, Rudels et al. (1996) found new halocline formation taking place when relatively fresh shelf waters near the surface were advected above denser and saltier water below, limiting winter convection, while Rudels et al. (2004) and Alkire et al. (2017) stressed the role of melt water in general (including non-shelf water) in the warm Atlantic inflow through the Fram Strait and the Barents Sea for halocline formation via this type of capping mechanism.~~ [Figure: 2](#) suggests that in this particular case, the convection ^{I.P}~~may have~~ affected halocline water^{I.P} ~~because prior to the onset of convection,~~
250 [Fig. 2 shows a well-defined halocline](#). This is also consistent with a study by Steele and Boyd (1998), who suggested that the ^{I.P}[winter convection and capping](#) mechanism can act in addition to the advection of dense and saline shelf waters. In the Steele and Boyd (1998) mechanism, which combines findings by Rudels et al. (1996) with earlier findings (e.g. Aagaard et al., 1981), high salinity in the capped water derives from advected cold and dense shelf water, which may previously have been affected by brine release in shelf seas, and not directly from AW. Here, the origin of the halocline water is unclear. However, Fig. [3oh](#)

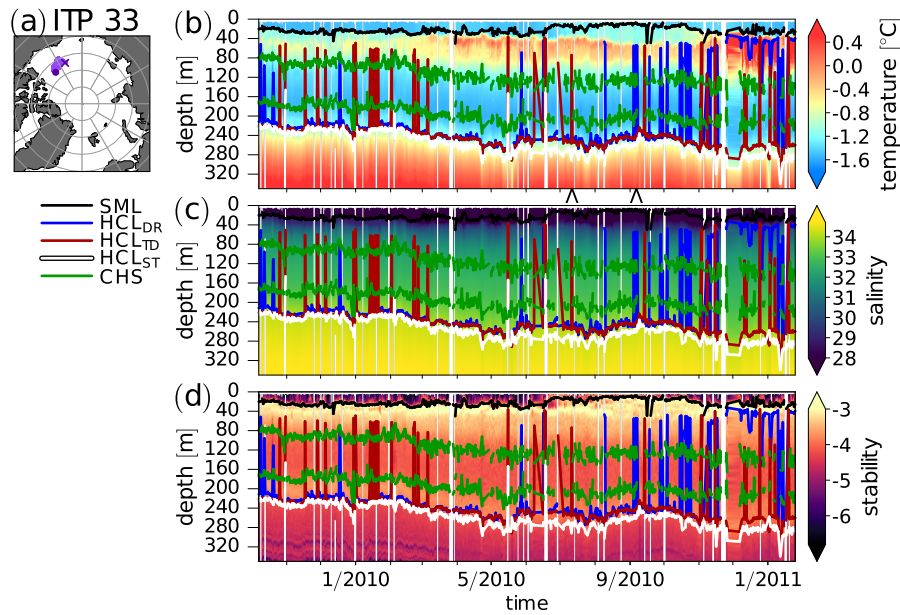


Figure 4. As Fig. 2 but for ITP-33. Additionally, the results of the cold halostad bound estimation are shown in dark green.

255 for 15 July 2014 (after winter convection) ^{LP}identifies a stability maximum associated with fresh water near the surface. This suggests that the ST method might indeed be useful for identifying the beginning of new halocline formation via the Rudels et al. (1996, 2004) ^{LP}convective homogenization and capping mechanism or the Steele and Boyd (1998) mechanism which essentially assumes that the Rudels et al. (1996) ^{LP}convective homogenization and capping mechanism acts in addition to the advection of dense shelf water (e.g. Aagaard et al., 1981).

260 Figure 4 again compares the three different methods for determining the halocline base depth, but this time for ITP-33, which drifted in the Canada Basin between October 2009 and January 2011, where it encountered PSW on top of PWW. In addition to the halocline base depth, Fig. 4b–d shows the CHS boundaries which have been estimated based on stability as described above. The performance of the new algorithm for identifying the CHS will be discussed further below. For now, the main focus will be on isolated spurious minima of the halocline base depth. As evidenced by the spikes in Fig. 4b–d, such isolated
 265 spurious base depth minima occur for the DR and the TD algorithm, but not the ST algorithm. ^{LP}Reasons for the occurrence of these artifacts will be further analyzed based on Figure 5. Figure 5a–~~ed~~ shows a case from ITP-33 on 11 July 2010 in which the TD method produced an isolated halocline base depth minimum and Fig. 5f–~~je–f~~ shows a case on 6 September 2010 in which the DR method produced an isolated halocline base depth minimum. In both cases, the isolated minima are related to a layer of warm PSW around ~80 m (Figs. 5a and ~~fe~~, compare also Fig. 4b). For 11 July 2010, the best estimate of the halocline
 270 base depth is provided by the DR method (Fig. 5~~cb~~). The DR method correctly places the base of the halocline water at a depth, where the salinity gradient ^{LP}(Fig. 5a) changes ^{LP}(Fig. 5a). Stability ^{LP}(Fig. 5d) also decreases markedly at this depth, although the ST method identifies the halocline base about 20 m below this location (Fig. 5~~ed~~). The TD method ^{LP}(Fig. 5e)

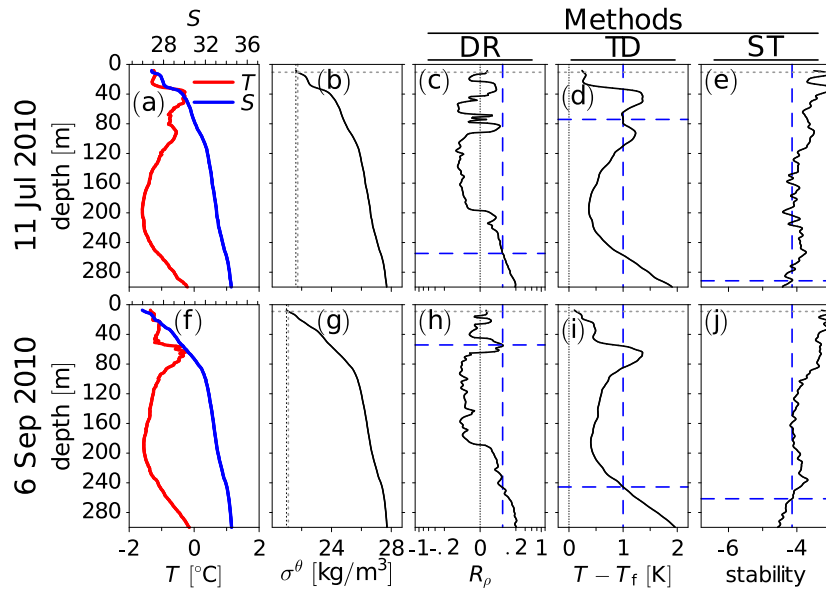


Figure 5. Please note: Added profiles of potential density anomaly and fixed overlapping labels. As Figure 3, but for two profiles from ITP-33. For 12 July 2010 [\(a-e\)](#)–[\(a-d\)](#) the TD method shows an isolated minimum of the halocline base depth, and for 6 September 2010 [\(f-j\)](#)–[\(e-f\)](#) the DRTD method shows an isolated minimum of the halocline base depth. ^{1P}[Supplement 6 shows a corresponding figure based on Level I data instead of the more processed Level III data.](#)

places the halocline base at about 80 m in the layer of warm PSW ^{1P}[\(Fig. 5d\)](#), although the salinity gradient below this layer still indicates the presence of a halocline and temperature decreases below this layer, indicating PWW. For 6 September 2010, the DR threshold is exceeded at a local density ratio maximum ^{1P}[\(Fig. 5h\)](#) which is related to a very steep temperature gradient ^{1P}[\(Fig. 5f\)](#) at the base of the PSW ^{1P}[\(Fig. 5f\)](#). While all three methods rely on finding a threshold, the search direction differs. Because the ST method searches upward, the warm PSW layer does not result in isolated depth minima (Figs. [5ed](#) and [jh](#)). Overall, this analysis suggests that the search direction matters ^{1P}[for whether spurious halocline base depth minima are detected or not](#). With the DR and the TD method, we search downward, while with the ST method we search upward. ^{1P}[Based on the stability profile in Fig. 5e, searching downward would lead to spurious depth minima in the ST method as well. This implies that the downward search direction in the ST method](#) This helps to explain why the ST method yields more robust results with fewer unexpected depth minima appearing in the basin-wise statistics discussed below. For the DR method, on the other hand, Fig. 3a shows that the DR threshold is exceeded also far below the halocline base. Such local DR maxima below the halocline base were also found in the presence of thermohaline staircases (not shown here). Additional DR maxima below the halocline base, such as the one in Fig. 3, prevent us from simply reversing the search direction in the DR algorithm.

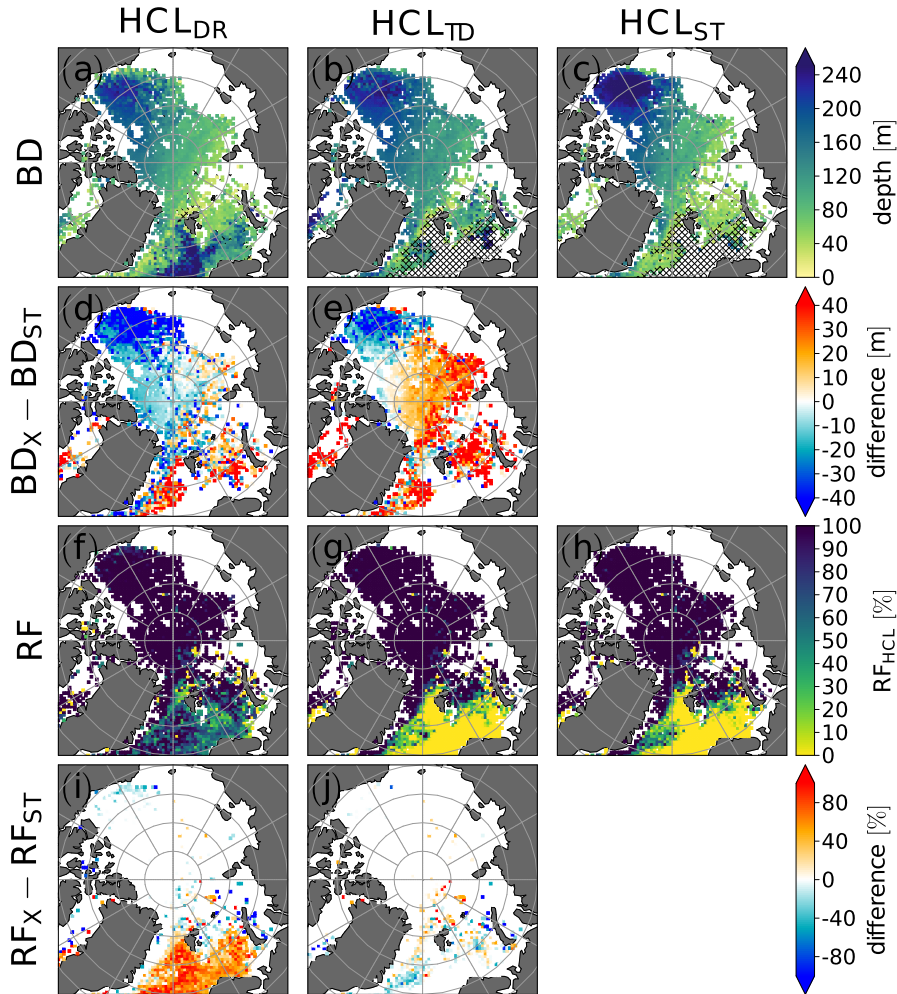


Figure 6. Halocline (HCL) base depth (BD) derived by the density-ratio (DR) algorithm (a), the temperature-difference (TD) algorithm (b), and the new stability (ST) algorithm (c). Difference of HCL BD between the DR and the ST algorithm (d) and between the TD and the ST algorithm (e). Relative frequency (RF) of HCL occurrence (i.e. number of profiles for which a halocline was detected divided by number of profiles analyzed) (f–h) and differences (i–j) as in (a–e). In (a–c), points where the relative occurrence frequency of the HCL was below 1% were masked out. Hatching indicates regions where the HCL occurrence frequency is below 25%. Points where the ocean floor depth is shallower than below 100 m were masked out.

3.2 Statistical comparison of the halocline base depth and occurrence frequency from different methods

In order to identify differences between the methods used for halocline base detection regarding the geographical distribution of halocline base depth and halocline occurrence frequency (i.e. number of profiles for which a halocline base was detected divided by number of profiles analyzed) we used a simple nearest-neighbor (NN) averaging to produce maps (Fig. 6). ^{1P}The

290 ~~underlying grid uses an azimuthal-equidistant projection with $\sim 0.47^\circ$ resolution at the North Pole.~~ In addition to these maps (which in data-rich regions show a time mean halocline base depth), we computed basin-wise statistics of halocline base depths. Figure 7 shows relative frequencies of halocline base depth diagnosed with the three methods for the Eurasian Basin, the Makarov Basin, and the Canada Basin.

As expected, all three methods yield a similar overall spatial distribution of halocline base depth ^{1.P}(Fig. 6a–c) with shallower
295 halocline base in the Eurasian Basin and the Makarov Basin compared to the Canada Basin ^{1.P} (Fig. 6a–c). This spatial pattern is consistent with Polyakov et al. (2018). In the Eurasian Basin, the time averaged halocline base depth diagnosed with the DR method (Fig. 6a) and the ST method (Fig. 6c) agree relatively well, while the TD method ^{1.P} ~~placed the overestimates~~ halocline
^{1.P} ~~at greater~~ depth ^{1.P} ~~compared relative~~ to both other methods (Fig. 6b). For the elliptical area covering the Eurasian Basin in
Fig. 7a, the mean base depth was 85.9 m for the DR method and 92.3 m for the ST method vs. 116.1 m for the TD method. This
300 ^{1.P} ~~greater overestimate of the~~ halocline base depth ^{1.P} ~~from~~ by the TD method compared to the other two methods is consistent with the previous result for ITP-74. Unlike the DR and the ST method, which both correctly identified the CHL base during the first months of ITP-74, the TD method placed the halocline base somewhere in the LHW.

In addition to the moderate difference in the mean base depth between the DR and the ST method, the relative frequency of halocline base depth ^{1.P}(Fig. 7b) in the Eurasian Basin reveals differences between the DR and the ST method, which are not
305 reflected by the difference of the mean base depths ^{1.P} (Fig. 7b). The ST method more often identifies a shallow halocline base (< 60 m) in the Eurasian Basin compared to the DR method, which is consistent with the finding that the ST method apparently captures the start of new halocline formation from Sect. 3.1. ^{M.A.} ~~The ST method also detects more frequent cases of halocline base depth below 120 m compared to the DR method~~ ~~More frequent detections of halocline bases not only above 60 m but also below 120 m with the ST method compared to the DR method account for a slightly wider halocline base depth distribution in~~
310 ~~the Eurasian Basin in the ST method compared to the DR method~~ (Fig. 7b). The more frequent halocline base depths larger than 120 m in the ST method are likely related to ^{1.P} ~~a deeper an overestimate of~~ halocline base ^{1.P} ~~depth~~ similar to the one found for the ST method for ITP-33 above. Slightly increasing the stability threshold in the ST method may lead to a better match between the halocline base depth estimate from the ST and the TD method by moving the halocline base estimated by the ST method upward and by decreasing the sensitivity of the ST method to new halocline formation. For the elliptical area covering
315 the Makarov Basin in Fig. 7b, the DR method yielded a mean halocline base depth of 112.3 m, the ST method of 118.1 m, and the TD method ^{M.A.} ~~again yielded a greater mean halocline base depth of~~ 133.5 m.

For the elliptical area covering the Canada Basin, on the other hand, the ST method yielded the largest mean halocline base depth. The mean halocline base depths for the Canada Basin corresponding to Fig. 7d are 191.4 m for the DR method, 206.6 m for the TD method, and 219.1 m for the ST method. In the Canada Basin ^{1.P} (Fig. 7d), the ST method detected a halocline base
320 shallower than 160 m for 0.05% of the profiles, while the DR method detected a halocline base shallower than 160 m for 10.2% of the profiles and the TD method for 3.5% of the profiles, indicative of isolated base depth minima due to the influence of warm PSW above PWW ^{1.P} (Fig. 7d). Isolated minima very likely also contribute to a more variable (noisier) halocline base depth in the Canada Basin in the map for the DR method in Fig. 6a and to a lesser extent also in the map for the TD method in Fig. 6b compared to the ST method (Fig. 6c). The larger average base depth in the Canada Basin in the ST method compared

325 to both other methods (see also Fig. 6d and e) is, however, not only explained by the isolated depth minima in the DR and
the TD method in Fig. 7d. Instead, more frequent depths greater than 260 m in the ST method compared to the other two
methods (Fig. 7d) contribute to the greater average halocline base depth diagnosed with the ST method, again indicating that a
slight increase of the stability threshold in the ST method would lead to a better agreement between the halocline base depth
from the ST and the DR method. While a halocline was almost always detected in the Canada Basin by all three methods, the
330 relative occurrence frequency (defined as the number of profiles in which a halocline base was detected divided by the total
number of profiles which were analyzed) varies strongly in the Norwegian Sea (Fig. 6f–h). While the ST method and also the
TD method very rarely detected a halocline base in the Norwegian Sea, the DR method frequently detected a halocline base
in the Norwegian Sea. Furthermore, the DR method suggests a transition from a deeper halocline in relatively warm water
inflow to a shallower halocline further north, which is absent in the other two methods (Fig. 6a–c). When using the DR method
335 for analyzing halocline retreat in these warm water inflow regions, this may lead to different results compared to the two
other methods. One reason for the DR method detecting a halocline base at depth could be thermohaline staircases. Overall,
the largest differences in halocline detection frequency between the methods (Fig. 6i and j) were found in regions which are
prone to sea ice retreat and, according to global climate model results, may also be particularly prone to events, in which large
temperature gradients are found directly underneath the SML, and which mainly occur during winter (Metzner et al., 2020). In
340 order to prevent the DR method from identifying a halocline base in relatively warm water, one could either limit the region
to which the method is applied (as Polyakov et al., 2018) or else introduce additional constraints on the water temperature.
Limiting the region is clearly a sensible choice in a stable climate. However, limiting the region to a region in which a stable
(cold) halocline is found at most times limits us in studying regional shifts. With regard to shifts due to climate change, one
should be aware that methods differ regarding requirements for halocline base identification and results.

345 3.3 Estimation of cold halostad boundaries

In the Canada Basin, the PWW forms a so-called cold halostad, while the LHW is modified water of Atlantic origin. This
leads to a local vertical stability minimum between two local vertical stability maxima (Fig. 5ed and jh). ^{1.P}~~The upper-vertical
stability maximum is associated with an increase of salinity near the top of the PWW and the lower stability maximum is
associated with an increase in salinity between PWW and LHW.~~ The local minimum of vertical stability between these two
350 local maxima is associated with a small salinity gradient around the core of the PWW (Fig. 5a and fe). ^{1.P}~~The new algorithm
described in Sect. 2.2 was designed to provide estimates for the location of the cold halostad layer boundaries and the center,
where the center is assumed to be the mean depth between the upper and the lower boundary.~~ Top and base depth timeseries
^{1.P}~~of the CHS~~ derived with the new algorithm ^{1.P}~~described in Sect. 2.2~~ are shown by dark green lines in Fig. 4. The algorithm
was designed to avoid misclassifications of the cold halostad by requiring the difference between the lower stability maximum
355 and the stability minimum (i.e. the depth of the 'stability valley') to be at least 0.2. Furthermore, the vertical extent of the
'stability valley' was required to be greater than 50m. This leads to occasional discontinuities in the cold halostad boundary.
Figure- 4 shows such discontinuities as evidenced by the breaks in the dark green lines. Furthermore, the requirement of a
minimum depth leads to shallow halostad layers not being detected.

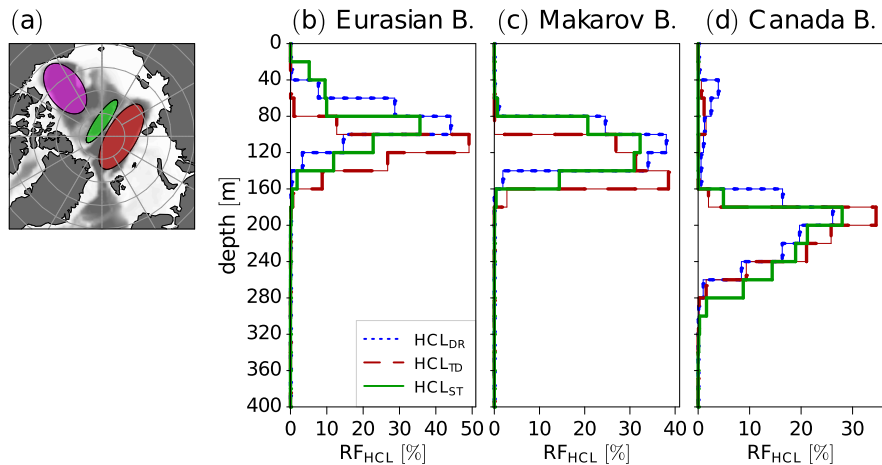


Figure 7. Please note: We made the profile plots taller. Map showing elliptical areas over the Canada Basin (purple), the Makarov Basin (green) and the Eurasian Basin (dark red) and ocean floor depth (grey shading) (a). Relative frequency of halocline (HCL) base depth determined with the density ratio (DR), temperature difference (DR) and the stability (ST) method for the elliptical areas over the Eurasian Basin (b), the Makarov Basin (c), and the Canada Basin (d).

Collecting all available observations with detected cold halostad boundaries per grid cell leads to the maps of CHS center depth and CHS thickness shown in Fig. 8a and b. The main occurrence region of the cold halostad is the Canada Basin, where Pacific water circulates between the SML and water of Atlantic origin (Shimada et al., 2005). Employing conservative assumptions to avoid a misclassification (including a lower bound of 50 m for the thickness), we detect a cold halostad layer in the Canada Basin region in Fig. 8b ~70–90% of the time, except in August, September, and October when the mean occurrence frequency ranges from slightly below 60% to slightly below 70% (Fig. 8c). ^{LP}Figures 8a and b show that in August, September, and October the fraction of grid points for which observations were available within the Canada Basin region was also particularly high (red line in Fig. 8c). Based on Fig. 1, more points at the edge of the Canada Basin region in Fig. 8b, where the occurrence frequencies decrease, may have been included in the analysis during these months. Furthermore, a cold halostad was ^{LP}also detected near the coasts of Greenland where glacial cold water acts similar to the Pacific low salinity water (Dmitrenko et al., 2017).

370 4 Summary and discussion

We introduced a new method for determining the halocline base depth based on vertical stability and compared it to the density ratio ^{M.A.}(DR) and the temperature difference ^{M.A.}(TD) method. Our main motivation for using a vertical stability ^{M.A.}(ST) threshold instead of a DR or TD threshold was that vertical stability is more closely related to the role of the halocline as a stable layer which separates the ^{M.A.}surface mixed layer SML from warmer ^{M.A.}Atlantic Water (AW^{M.A.}) below and thus acts

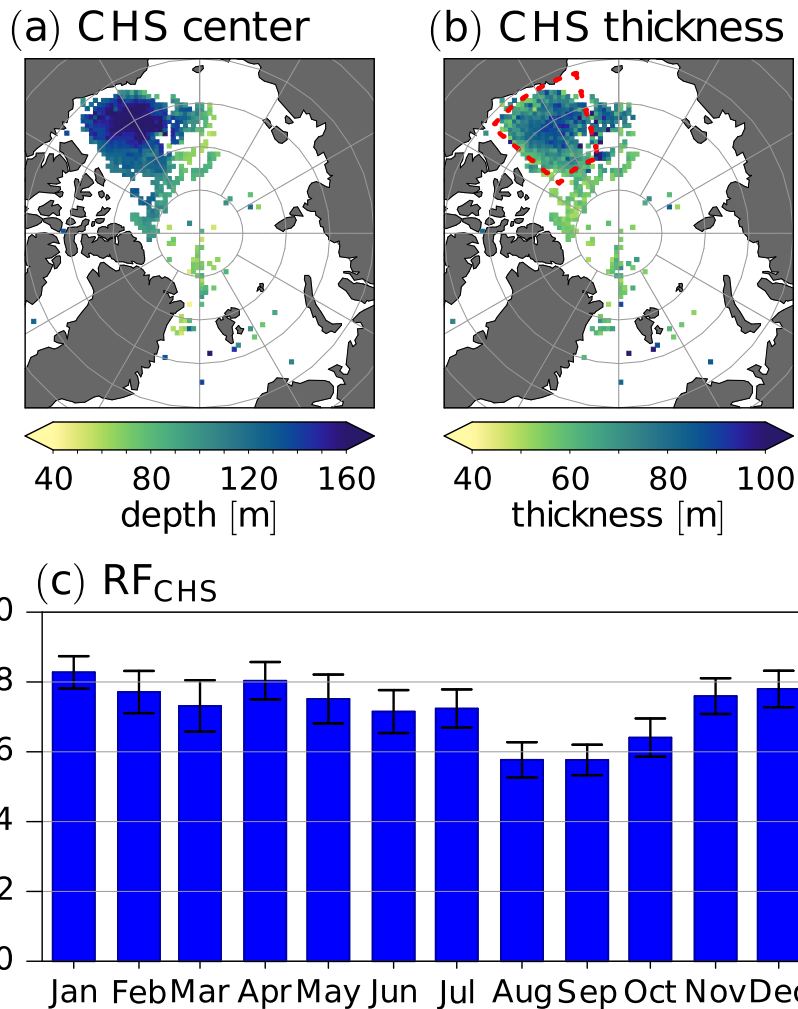


Figure 8. Please note: Figure 8c was revised to show 95% confidence intervals for the mean. The fraction of grid points for which at least one observation was available in the respective month was omitted. The panels were enlarged and rearranged. The color bars on the maps are now oriented horizontally instead of vertically. Maps of mean (a) CHS center depth (a) and (b) CHS thickness (b). (c) Monthly relative occurrence frequency (RF_{CHS}^{IP}, blue bars) of the CHS in the Canada Basin region (area enclosed by red dashed lines in ^{IP}b) and 95% confidence interval for the mean (c)(b) and fraction of grid points (FG) for which at least one observation was available in the respective month (red line).

375 to protect sea ice. Another objective was to design a particularly robust method ^{M.A.}with few artifacts. ^{IP}Furthermore, the new ST algorithm does not require masking out pre-defined geographical regions solely based on their location. This is important because in a climate change context, the location of water masses may shift as the Arctic warms or cools. We also devised a new stability-based method to identify the ^{M.A.}cold halostad (CHS^{M.A.}), which is formed by ^{M.A.}Pacific Winter Water (PWW^{M.A.})

in the Canada Basin and also by melt water off the eastern coast of Greenland and Svalbard. To our knowledge, this is the first
380 time that a method for detecting the CHS has been devised and tested.

We found that the DR and the new ST method both correctly identified the base of the ^{M.A.}cold halocline layer~~CHL~~ in
the Eurasian Basin during the first months of ITP-74, while the TD method placed the halocline base somewhere in the
^{M.A.}lower halocline water~~LHW~~. ~~T~~Furthermore, the analysis of individual profiles after convection in ITP-74 indicated that the
new ST method captured the beginning of new halocline formation via the convective homogenization and subsequent fresh
385 water capping mechanism proposed by Rudels et al. (1996). In the Canada Basin, the new method ^{I.P.}~~placed~~overestimated the
halocline base ^{I.P.}~~deeper than~~depth compared to the DR method, which correctly identified the halocline base for ITP-33. This
disagreement between the DR and the ST method could be reduced by slightly increasing the stability threshold in the ST
method. Slightly increasing the stability threshold (which is at present based on an approximate relationship between density
ratio and stability) may lead to a better agreement of halocline base depth between the DR and the ST method not only by
390 moving the halocline base from the ST method upward but also by decreasing the sensitivity of the ST method to new halocline
formation. ^{M.A.}However, instead of simply aiming for a better match between the ST and the DR method, it may ultimately be
more desirable to further fine tune the ST threshold based on an empirical analysis of profiles, similar to how Bourgain and
Gascard (2011) determined the DR threshold. On the whole, estimating the ST threshold based on the DR threshold as we did
provides fairly reasonable results, even without further fine tuning.

395 Unlike the two existing methods, the new ST method to detect the halocline base yielded few artificial halocline base depth
minima. In the two existing methods, such artifacts were found to be associated with warm ^{M.A.}Pacific Summer Water~~PSW~~ on
top of cold PWW in the Canada Basin. Because the new method searches for the halocline base from below, such artifacts were
avoided, leading to a more robust method, especially compared to the widely used DR method. Unfortunately, because of DR
maxima below the cold halocline base (which are for example associated with thermohaline staircases), the search direction in
400 the DR method cannot simply be reversed in order to increase the robustness also of the DR method.

A particularly striking difference between the DR method and the other two methods was found in the Norwegian Sea.
While the ST and the TD method almost never detected a halocline in the Norwegian Sea, the DR method frequently detected
a halocline base in the Norwegian Sea. Remarkably, the halocline in the DR method decreased north of the Norwegian Sea.
This intriguing difference between the methods should be taken into account, for example when studying the effects of warm
405 AW inflow on the cold halocline, especially because warm water inflow regions are particularly prone to react to anthropogenic
warming (although the effects of warming on either accelerating or preventing new halocline formation are manifold and
changing over time, and destabilization of an existing stable halocline by warming from below is only one potential contributor
to increased annual mean net surface heat fluxes from the ocean to the atmosphere in warm water inflow regions found in
climate models).

410 Regarding the new method for CHS detection, a case study and an application to a comprehensive dataset yielded encourag-
ing results. The case study suggested that the method correctly identified a layer with a small vertical salinity gradient formed
by PWW. This small salinity gradient led to a stability minimum between two local stability maxima which was captured by the
new stability method for CHS detection. Because we found it necessary to introduce a constraint on the cold halostad thickness

and to set a threshold requirement for the magnitude of the stability minimum, our method suffers from a low detection sensitiv-
415 ity and altogether misses cold halostad layers that are thinner than 50 m. Nevertheless, a cold halostad was frequently detected
in the Canada Basin throughout the year and the number of missed detections tended to be small as for ITP-33^{M.A.} albeit with
detection rates varying across ITPs tested from almost perfect to a slightly higher mismatch rate, while some other ITPs yielded
almost perfect results and some other ITPs slightly worse results (not shown). This suggests that ^{M.A.} the new stability-based
method for CHS detection could be useful for future studies exploring variability and changes of the CHS in the Canada Basin.

420 One method to advance cold halostad and halocline base detection in the future may lie in the application of artificial
intelligence. This would require a-priori manual classification applied to a training and an evaluation dataset. In the absence
of objective criteria that work under most circumstances, such manual classification would ultimately have to rely on expert
judgment, which may in turn introduce a different set of problems. ^{M.A.} Rapid advances in AI may help to overcome these
problems. Given the various shortcomings of traditional threshold methods, AI-based methods could nevertheless be useful.

425 *Code and data availability.* The Ice tethered profiler data (Krishfield et al., 2008; Toole et al., 2011) used in this paper are taken from
the website of the Ice-Tethered Profiler program based on Woods Hole Oceanic institution via <https://www2.whoi.edu/site/itp/> (last access
23 January 2022). The UDASH-dataset (Behrendt et al., 2018) is available from the PANGAEA data archive at [http://doi.org/10.1594/
PANGAEA.872931](http://doi.org/10.1594/PANGAEA.872931). Sea ice data in Supplement 5 was obtained from <https://www.meereisportal.de>.

Author contributions. E.P.M. devised the new method for determining the Arctic Ocean cold halocline and cold halostad layer depths and
430 performed the data analysis. Both authors contributed equally to writing the manuscript.

Competing interests. The authors declare that they have no conflict of interest.

Acknowledgements. We thank the two reviewers, I. Polyakov and M. Athanase, for their very insightful and very constructive comments,
especially for their suggestions regarding the analysis of individual profiles, new halocline formation, the structure of the introduction, and
basin-wise statistics, which we consider a major contribution to our revised manuscript. The Ice-Tethered Profiler data were collected and
435 made available by the Ice-Tethered Profiler Program based at the Woods Hole Oceanographic Institution (<http://www2.whoi.edu/site/itp/>). Sea
ice data in Supplement 5 was obtained from <https://www.meereisportal.de> (Grosfeld et al., 2016, funded by REKLIM-2013-04). We gratefully
acknowledge the funding by the Deutsche Forschungsgemeinschaft (DFG, German Research Foundation) - Projektnummer 268020496
- TRR 172, within the Transregional Collaborative Research Center "Arctic Amplification: Climate Relevant Atmospheric and Surface
Processes, and Feedback Mechanisms (AC)³". We thank J. Chylik for comments that helped to improve the readability of our manuscript.

440 References

- Aagaard, K., Coachman, L. K., and Carmack, E.: On the halocline of the Arctic Ocean, *Deep Sea Res. Part I Oceanogr. Res. Pap.*, 28, 529–545, [https://doi.org/10.1016/0198-0149\(81\)90115-1](https://doi.org/10.1016/0198-0149(81)90115-1), 1981.
- Alkire, M. B., Polyakov, I., Rember, R., Pnyushkov, A., Ivanov, V., and Ashik, I.: Combining physical and geochemical methods to investigate lower halocline water formation and modification along the Siberian continental slope, *Ocean Sci.*, 13, 983–995, <https://doi.org/10.5194/os-13-983-2017>, 2017.
- Anderson, L. G., Andersson, P. S., Björk, G., Jones, E. P., Jutterström, S., and Wåhlström, I.: Source and formation of the upper halocline of the Arctic Ocean, *J. Geophys. Res. Oceans*, 118, 410–421, <https://doi.org/10.1029/2012jc008291>, 2013.
- Athanase, M.: ^{MA and LP}~~Review on the manuscript EGUSPHERE-2023-106~~, *EGUsphere*, <https://doi.org/10.5194/egusphere-2023-106-RC2>, 2023.
- 450 Behrendt, A., Sumata, H., Rabe, B., and Schauer, U.: UDASH – Unified Database for Arctic and Subarctic Hydrography, *Earth Syst. Sci. Data*, 10, 1119–1138, <https://doi.org/10.5194/essd-10-1119-2018>, 2018.
- Bertosio, C., Provost, C., Sennéchaël, N., Artana, C., Athanase, M., Boles, E., Lellouche, J.-M., and Garric, G.: The western Eurasian Basin halocline in 2017: Insights from autonomous NO measurements and the Mercator Physical System, *J. Geophys. Res. Oceans*, 125, e2020JC016204, <https://doi.org/10.1029/2020JC016204>, 2020.
- 455 Bertosio, C., Provost, C., Athanase, M., Sennéchaël, N., Garric, G., Lellouche, J.-M., Kim, J.-H., Cho, K.-H., and Park, T.: Changes in Arctic halocline waters along the East Siberian Slope and in the Makarov Basin from 2007 to 2020, *J. Geophys. Res. Oceans*, 127, <https://doi.org/10.1029/2021jc018082>, 2022.
- Björk, G., Söderkvist, J., Winsor, P., Nikolopoulos, A., and Steele, M.: Return of the cold halocline layer to the Amundsen Basin of the Arctic Ocean: Implication for the sea ice mass balance, *Geophys. Res. Lett.*, 29, 1–8, <https://doi.org/10.1029/2001GL014157>, 2002.
- 460 Bourgain, P. and Gascard, J. C.: The Arctic Ocean halocline and its interannual variability from 1997 to 2008, *Deep Sea Res. Part I Oceanogr. Res. Pap.*, 58, 745–756, <https://doi.org/10.1016/j.dsr.2011.05.001>, 2011.
- Deng, G. and Cahill, L.: An adaptive Gaussian filter for noise reduction and edge detection, in: 1993 IEEE Conference Record Nuclear Science Symposium and Medical Imaging Conference, vol. 3, pp. 1615–1619, IEEE, San Francisco, CA, USA, <https://doi.org/10.1109/nssmic.1993.373563>, 1993.
- 465 Dmitrenko, I. A., Kirillov, S. A., Rudels, B., Babb, D. G., Pedersen, L. T., Rysgaard, S., Kristoffersen, Y., and Barber, D. G.: Arctic Ocean outflow and glacier–ocean interactions modify water over the Wandel Sea shelf (northeastern Greenland), *Ocean Sci.*, 13, 1045–1060, <https://doi.org/10.5194/os-13-1045-2017>, 2017.
- GEBCO Bathymetric Compilation Group 2021: The GEBCO_2021 grid - a continuous terrain model of the global oceans and land., <https://doi.org/10.5285/c6612cbe-50b3-0cff-e053-6c86abc09f8f>, 2021.
- 470 Gill, A. E.: *Atmosphere-ocean dynamics* (International Geophysics Series, Volume 30), Academic Press, 1982.
- Grosfeld, K., Treffeisen, R., Asseng, J., Bartsch, A., Bräuer, B., Fritsch, B., Gerdes, R., Hendricks, S., Hiller, W., Heygster, G., Krumpen, T., Lemke, P., Melsheimer, C., Nicolaus, M., Ricker, R., and Weigelt, M.: [Online Sea-Ice Knowledge and Data Platform](#), *Polarforschung*; 85, <https://doi.org/10.2312/POLFOR.2016.011>, 2016.
- Janzen, C., Larson, N., and Murphy, D.: ^{LP}[Long-term accuracy, stability of Argo CTDs](#), *Sea Technology*, 2016.
- 475 Jones, E. P. and Anderson, L. G.: On the origin of the chemical properties of the Arctic Ocean halocline, *J. Geophys. Res.*, 91, 10759, <https://doi.org/10.1029/jc091ic09p10759>, 1986.

- Krishfield, R., Toole, J., Proshutinsky, A., and Timmermans, M.-L.: Automated ice-tethered profilers for seawater observations under pack ice in all seasons, *J. Atmos. Ocean Technol.*, 25, 2091–2105, <https://doi.org/10.1175/2008JTECHO587.1>, 2008.
- 480 Lind, S., Ingvaldsen, R. B., and Furevik, T.: Arctic layer salinity controls heat loss from deep Atlantic layer in seasonally ice-covered areas of the Barents Sea, *Geophys. Res. Lett.*, 43, 5233–5242, <https://doi.org/10.1002/2016GL068421>, 2016.
- Macdonald, R. W., Kuzyk, Z. A., and Johannessen, S. C.: It is not just about the ice: a geochemical perspective on the changing Arctic Ocean, *J. Environ. Stud. Sci.*, 5, 288–301, <https://doi.org/10.1007/s13412-015-0302-4>, 2015.
- McDougall, T. J., Feistel, R., Wright, D. G., Pawlowicz, R., Millero, F. J., Jackett, D. R., King, B. A., Marion, G. M., Seitz, S., Spitzer, P., and Chen, C.-T.: ^{1P}[The international thermodynamic equation of seawater – 2010: Calculation and use of thermodynamic properties](#), *Intergovernmental Oceanographic Commission, Manuals and Guides No. 56, UNESCO*, <https://doi.org/10.25607/OBP-1338>, 2010.
- 485 Metzner, E. P., Salzmann, M., and Gerdes, R.: Arctic Ocean surface energy flux and the cold halocline in future climate projections, *J. Geophys. Res. Oceans*, 125, e2019JC015 554, <https://doi.org/10.1029/2019JC015554>, 2020.
- Peralta-Ferriz, C. and Woodgate, R. A.: Seasonal and interannual variability of pan-Arctic surface mixed layer properties from 1979 to 2012 from hydrographic data, and the dominance of stratification for multiyear mixed layer depth shoaling, *Prog. Oceanogr.*, 134, 19–53, <https://doi.org/10.1016/j.pocean.2014.12.005>, 2015.
- 490 Polyakov, I.: ^{MA and 1P}[Review of the manuscript \(egusphere-2023-106\) entitled “Technical note: Determining Arctic Ocean cold halocline and cold halostad layer depths based on vertical stability” by E. P. Metzner and M. Salzmann](#), *EGUsphere*, <https://doi.org/10.5194/egusphere-2023-106-RC1>, 2023.
- Polyakov, I. V., Pnyushkov, A. V., Alkire, M. B., Ashik, I. M., Baumann, T. M., Carmack, E. C., Goszczko, I., Guthrie, J., Ivanov, V. V., 495 Kanzow, T., Krishfield, R., Kwok, R., Sundfjord, A., Morison, J., Rember, R., and Yulin, A.: Greater role for Atlantic inflows on sea-ice loss in the Eurasian Basin of the Arctic Ocean, *Science*, 356, <https://doi.org/10.1126/science.aai8204>, 2017.
- Polyakov, I. V., Pnyushkov, A. V., and Carmack, E. C.: Stability of the Arctic halocline: a new indicator of Arctic climate change, *Environ. Res. Lett.*, 13, <https://doi.org/10.1088/1748-9326/aaec1e>, 2018.
- Polyakov, I. V., Rippeth, T. P., Fer, I., Alkire, M. B., Baumann, T. M., Carmack, E. C., Ingvaldsen, R., Ivanov, V. V., Janout, M., Lind, S., 500 Padman, L., Pnyushkov, A. V., and Rember, R.: Weakening of cold halocline layer exposes sea ice to oceanic heat in the eastern Arctic Ocean, *J. Clim.*, 33, 8107–8123, <https://doi.org/10.1175/JCLI-D-19-0976.1>, 2020.
- Roquet, F., Ferreira, D., Caneill, R., Schlesinger, D., and Madec, G.: Unique thermal expansion properties of water key to the formation of sea ice on Earth, *Sci. Adv.*, 8, <https://doi.org/10.1126/sciadv.abq0793>, 2022.
- Rudels, B., Anderson, L. G., and Jones, E. P.: Formation and evolution of the surface mixed layer and halocline of the Arctic Ocean, *J. Geophys. Res. Oceans*, 101, 8807–8821, <https://doi.org/10.1029/96JC00143>, 1996.
- 505 Rudels, B., Jones, E. P., Schauer, U., and Eriksson, P.: Atlantic sources of the Arctic Ocean surface and halocline waters, *Polar Res.*, 23, 181–208, <https://doi.org/10.3402/polar.v23i2.6278>, 2004.
- Shimada, K., Itoh, M., Nishino, S., McLaughlin, F., Carmack, E., and Proshutinsky, A.: Halocline structure in the Canada Basin of the Arctic Ocean, *Geophys. Res. Lett.*, 32, <https://doi.org/10.1029/2004GL021358>, 2005.
- 510 Shimada, K., Kamoshida, T., Itoh, M., Nishino, S., Carmack, E., McLaughlin, F., Zimmermann, S., and Proshutinsky, A.: ^{1P}[Pacific Ocean inflow: Influence on catastrophic reduction of sea ice cover in the Arctic Ocean](#), *Geophys. Res. Lett.*, 33, <https://doi.org/10.1029/2005gl025624>, 2006.
- Spreen, G., Kaleschke, L., and Heygster, G.: [Sea ice remote sensing using AMSR-E 89-GHz channels](#), *J. Geophys. Res.*, 113, <https://doi.org/10.1029/2005jc003384>, 2008.

- 515 Steele, M. and Boyd, T.: Retreat of the cold halocline layer in the Arctic Ocean, *J. Geophys. Res.*, 103, 10419–10435, <https://doi.org/10.1029/98JC00580>, 1998.
- Steele, M., Morison, J., and Curtin, T.: Halocline water formation in the Barents Sea, *J. Geophys. Res.*, 100, 881–894, 1995.
- Timmermans, M.-L., Proshutinsky, A., Golubeva, E., Jackson, J. M., Krishfield, R., McCall, M., Platov, G., Toole, J., Williams, W., Kikuchi, T., and Nishino, S.: Mechanisms of Pacific Summer Water variability in the Arctic's Central Canada Basin, *J. Geophys. Res. Oceans*, 119, 7523–7548, <https://doi.org/10.1002/2014jc010273>, 2014.
- 520 Toole, J. M., Krishfield, R. A., Timmermans, M.-L., and Proshutinsky, A.: The ice-tethered profiler: ARGO of the Arctic, *Oceanography*, 24, 126–135, <http://www.jstor.org/stable/24861307>, 2011.
- Wong, A., Keeley, R., Carval, T., and Argo Data Management Team: ^{1P}[Argo quality control manual for CTD and trajectory data](#), Tech. rep., <https://doi.org/doi.org/10.13155/33951>, 2023a.
- 525 Wong, A. P. S., Gilson, J., and Cabanes, C.: ^{1P}[Argo salinity: bias and uncertainty evaluation](#), *Earth Syst. Sci. Data*, 15, 383–393, <https://doi.org/10.5194/essd-15-383-2023>, 2023b.
- Zhong, W., Steele, M., Zhang, J., and Cole, S. T.: ^{M.A.}[Circulation of Pacific Winter Water in the Western Arctic Ocean](#), *J. of Geophys. Res. Oceans*, 124, 863–881, <https://doi.org/10.1029/2018jc014604>, 2019.